Differences in the management of intracellular redox state between wine yeast species dictate their fermentation performances and metabolite production.

Viwe Tyibilika, Mathabatha E. Setati, Audrey Bloem, Benoit Divol, Carole Camarasa

International Journal of Food Microbiology

Differences in the management of intracellular redox state between wine yeast species dictate their fermentation performances and metabolite production.

--Manuscript Draft--

Manuscript Number:	
Article Type:	Full Length Article
Keywords:	wine fermentation; Saccharomyces and non-Saccharomyces yeasts; redox homeostasis; NAD(H) and NADP(H); yeast redox metabolism
Corresponding Author:	Carole Camarasa French National Institute for Agricultural Research INRAE Montpellier, FRANCE
First Author:	Viwe Tyibilika
Order of Authors:	Viwe Tyibilika
	Mathabatha E. Setati
	Audrey Bloem
	Benoit Divol
	Carole Camarasa
Abstract:	The maintenance of the balance between oxidized and reduced redox cofactors is essential for the functioning of many cellular processes in all living organisms. During Saccharomyces cerevisiae fermentation, it is supported by metabolism and consequently, modulates the formation of a wide range of by-products. In this study, we investigated the question of variability between wine yeast species in their management of redox balance and its consequences on the fermentation performances and the formation of metabolites. To this aim, we quantified the changes in NAD(H) and NADP(H) concentrations and redox status throughout the fermentation of 6 wine yeast species. While the availability of NADP and NADPH remained balanced and stable throughout the process for all the strains, important differences between species were observed in the dynamics of NAD and NADH intracellular pools. A comparative analysis of these data with the fermentation capacity and metabolic profiles of the strains revealed that Saccharomyces cerevisiae, Torulaspora delbrueckii and Lachancea thermotolerans strains were able to reoxidize NADH to NAD throughout the fermentation, mainly by the formation of glycerol. These species exhibited good fermentation capacities. Conversely, Starmerella bacillaris and Metschnikowia pulcherrima species were unable to regenerate NAD as early as one third of sugars were consumed, explaining at least in part their poor growth and fermentation performances. The Kluyveromyces marxianus strain exhibited a specific behaviour, by maintaining similar levels of NAD and NADH throughout the process. This balance between oxidised and reduced redox cofactors ensured the consumption of a large part of sugars by this species, despite a low fermentation rate. In addition, the dynamics of redox cofactors affected the production of by-products by the various strains either directly or indirectly, through the formation of precursors. Major examples are the increased formation of glycerol by S. bacillaris and M. pulcherrima strains, as a way of trying to reoxidise NADH, and the greater capacity to produce acetate and derived metabolites of yeasts capable of maintaining their redox balance. Overall, this study provided new insight into the contribution of the management of redox status to the orientation of yeast metabolism during fermentation. This information should be taken into account when developing strategies for more efficient and effective fermentation.
Suggested Reviewers:	Jose Manuel Guillamon guillamon@iata.csic.es
	Vasileios Englezos vasileios.englezos@unito.it
	Andreas Gombert

	gombert@unicamp.br
	Pascale Daran-Lapujade p.a.s-daran-lapujade@tudelft.nl

Dr Carole Camarasa
UMR Sciences pour l'œnologie
INRAE- Montpellier

Dear Editor,

We are pleased to submit the attached manuscript titled "Differences in the management of intracellular redox state between wine yeast species dictate their fermentation performances and metabolite production" for consideration for publication in *International Journal of Food Microbiology*.

In recent years, innovative and more sustainable strategies have to be developed to respond to changes in consumer requirements and to meet the current challenges of the winemaking sector. The distinctive phenotypic traits of non-*Saccharomyces* yeast species has led to increased interest in considering it as a promising alternative. More widespread and efficient use of these yeasts is restricted, however, because of insufficient knowledge of its metabolic behaviour and no clear understanding of the similarities and differences to *S. cerevisiae*. In this context, we investigated how different wine yeast species manage the maintenance of redox balance and the consequences for their performance in fermentation.

In this work, through the comparison of the redox status dynamics, fermentation performances and production of metabolites, we demonstrate that the inability of some yeast strains to re-oxidize the reduced cofactor NADH explains, at least in part, their poor fermentation capacity. Furthermore, differences between wine yeast species in their redox state and its dynamics during fermentation are responsible, directly or indirectly, for their distinctive profile of central carbon metabolites and volatile compounds.

This paper provides essential knowledge that should be considered in order to exploit the phenotypic potential offered by non-*Saccharomyces* yeast in winemaking and more widely in the food and beverage industry. Overall, the findings reported in this study improve our knowledge on yeast physiology in the context of food fermentation, one of the main focuses of the *International Journal of Food Microbiology*.

We confirm that this manuscript has not been published elsewhere and is not under consideration by any other journal. All the authors have read and approved the manuscript, have significantly contributed to the paper, and agree with its submission to *International Journal of Food Microbiology*. We have no conflicts of interest to declare.

Thank you for your consideration. We hope that the *International Journal of Food Microbiology* journal will consider this study and look forward to your comments and feedback.

Yours sincerely,

Carole Camarasa

science for people, life & earth

UMR 1083 Sciences pour l'œnologie
2 place Viala
34060 Montpellier, France
Tel.: +33 1 (0)4 99 61 22 74

Join us
www6.montpellier.inrae.fr/spo/

Highlights

Intracellular NAD(H) pool and ratio vary during fermentation, contrary to NADP(H).

Yeast species vary in their ability to reoxidize NADH cofactors.

NAD^+/NADH imbalance alters yeast growth and fermentation performances.

Aroma compounds production in yeasts is a consequence of redox status of the cells.

Differences in the management of intracellular redox state between wine yeast species dictate their fermentation performances and metabolite production.

Viwe Tyibilika[1,2], Mathabatha E. Setati[2], Audrey Bloem[1], Benoit Divol[2], Carole Camarasa[1,2,*]

[1]UMR SPO, INRAE, Institut Agro, Université de Montpellier, Montpellier, France

[2]South African Grape and Wine Research Institute, Department of Viticulture and Oenology, Stellenbosch University, Private Bag X1, Matieland 7602, South Africa

*Corresponding author.

Email address: carole.camarasa@inrae.fr

Abstract

The maintenance of the balance between oxidized and reduced redox cofactors is essential for the functioning of many cellular processes in all living organisms. During *Saccharomyces cerevisiae* fermentation, it is supported by metabolism and consequently, modulates the formation of a wide range of by-products. In this study, we investigated the question of variability between wine yeast species in their management of redox balance and its consequences on the fermentation performances and the formation of metabolites. To this aim, we quantified the changes in NAD(H) and NADP(H) concentrations and redox status throughout the fermentation of 6 wine yeast species. While the availability of NADP and NADPH remained balanced and stable throughout the process for all the strains, important differences between species were observed in the dynamics of NAD and NADH intracellular pools. A comparative analysis of these data with the fermentation capacity and metabolic profiles of the strains revealed that *Saccharomyces cerevisiae*, *Torulaspora delbrueckii* and *Lachancea thermotolerans* strains were able to reoxidize NADH to NAD throughout the fermentation, mainly by the formation of glycerol. These species exhibited good fermentation capacities. Conversely, *Starmerella bacillaris* and *Metschnikowia pulcherrima* species were unable to regenerate NAD as early as one third of sugars were consumed, explaining at least in part their poor growth and fermentation performances. The *Kluyveromyces marxianus* strain exhibited a specific behaviour, by maintaining similar levels of NAD and NADH throughout the process. This balance between oxidised and reduced redox cofactors ensured the consumption of a large part of sugars by this species, despite a low fermentation rate. In addition, the dynamics of redox cofactors affected the production of by-products by the various strains either directly or indirectly, through the formation of precursors. Major examples are the increased formation of glycerol by *S. bacillaris* and *M. pulcherrima* strains, as a way of trying to reoxidise NADH, and the greater capacity to produce acetate and derived metabolites of yeasts capable of maintaining their redox balance. Overall, this study provided new insight into the contribution of the management of redox status to the orientation of yeast metabolism during fermentation. This information should be taken into account when developing strategies for more efficient and effective fermentation.

Keywords: wine fermentation, *Saccharomyces* and non-*Saccharomyces* yeasts, redox homeostasis, NAD(H) and NADP(H), yeast redox metabolism

1. Introduction

Yeasts have long been recognized for their role in fermenting sugars (Anderson, 1989; Gonzalez et al., 2021; Nielsen, 2003). During fermentation, they use the nutrients contained in grape juice for the generation of energy and the production of anabolic precursors, required for their growth and survival. In doing so, they convert sugars into ethanol and carbon dioxide as well as a wide range of metabolites including glycerol, organic acids and volatile compounds. The activity of this metabolic network is influenced by several factors including nutrient and substrate availability, oxygen requirements, and fermentation by-products (Barrajón-Simancas et al., 2011; Carrau et al., 2010, 2008; Fleet, 2003; Swiegers et al., 2005; Torrea, 2003). Several pathways of this network involve intricate reductive and oxidative reactions facilitated by dehydrogenase enzymes (about 200 reactions in *Saccharomyces cerevisiae*) that utilize nicotinamide adenine dinucleotide NAD(H) and its phosphorylated version NADP(H), as well as flavin adenine dinucleotide FAD(H_2) as cofactors (Nielsen, 2003). During fermentation, the formation of energy achieved by converting sugars into ethanol via glycolysis is a redox-neutral process. On the other hand, the formation of biomass (anabolism) and organic acids from sugars generates an excess of reduced cofactors NADH (Oura, 1977). Furthermore, anabolism is associated with the consumption of NADPH, used as reducing cofactor in many reactions involved in the biosynthesis of amino acids, lipids and nucleotides (Bruinenberg et al., 1983; Cortassa et al., 1995; van Dijken and Scheffers, 1986).

Maintaining cellular redox balance between oxidised and reduced cofactors is essential to ensuring metabolic functioning, but it is subjected to specific constraints during yeast fermentation. Importantly, *S. cerevisiae* and more generally wine yeasts do not possess any transhydrogenase enzyme for interconverting NADH and NADPH (Bruinenberg et al., 1983; Kulkarni and Brookes, 2019; Påhlman et al., 2001; Rigoulet et al., 2004; van Dijken and Scheffers, 1986; van Hoek and Merks, 2012a). Thus, exchanges between the two pyridine nucleotide coenzyme systems can only be ensured by the coupling of kinase and dehydrogenase activities, which enables the conversion of NADH and NADP cofactors into NAD and NADPH (Bakker et al., 2001; Nissen et al., 2001; Sazanov and Jackson, 1994). However, the actual contribution of these systems as redox shunt is minimal (Haselbeck and McAlister-Henn, 1993; Outten, 2003). In addition, the mitochondrial inner membrane is almost physically impermeable to redox cofactors (Jagow and Klingenberg, 1970). This imposes a separate management of the NADH and NADPH turnover in the different cellular compartments.

The amount of oxygen in natural grape juice is low, around 8 mg/L, and it is rapidly depleted, thereby rendering the medium anaerobic. Consequently, intracellular redox homeostasis during wine

fermentation is exclusively ensured through the production of ethanol and other metabolic end-products. In *S. cerevisiae,* the reduction of dihydroxyacetone-3-phosphate to glycerol-3-phosphate has been reported as the main route for balancing the cytosol surplus of NADH, while mitochondrial redox shuttles that export redox equivalents to the cytosol play a key role in mitochondrial NADH recycling (Bakker et al., 2001). NADPH consumption takes place mainly in the cytoplasm (Albers et al., 1998), and is largely compensated by the activity of the two dehydrogenases in the oxidative part of the pentose phosphate pathway: the glucose-6-phosphate dehydrogenase Zwf1p and the 6-phosphogluconate dehydrogenase Gnd1p. In addition, cytosolic (Ald6p) and mitochondrial (Ald4p, Ald5p) NADP-dependent aldehyde dehydrogenases fine-tune the NADPH turnover (Saint-Prix et al., 2004). In this context, previous works highlighted that *S. cerevisiae* redox metabolism exhibits remarkable flexibility, responding to external factors that modulate anabolic requirements by adjusting specific inter-compartmental electron exchanges and the formation of unique metabolites, while also facilitating the excretion of redox sinks (Hazelwood et al., 2008; Henriques et al., 2021; Nielsen, 2003; van Hoek and Merks, 2012b). This plasticity was also highlighted by altering NAD^+/NADH and $NADP^+$/NADPH ratios, which forced the yeast to redistribute the carbon flux in the metabolic network to restore the redox balance (Bloem et al., 2016; Celton et al., 2012a; Heux et al., 2006; Hou et al., 2009; Jain et al., 2012). Apart from influencing the formation of central carbon metabolites, this metabolic flexibility to maintain redox balance modulates the synthesis of other compounds involving dehydrogenases (Bloem et al., 2016; Celton et al., 2012b, 2012a; Duncan et al., 2023; Jain et al., 2012). These include a variety of aroma and flavour compounds of interest for the sensory quality of fermented beverages.

Non-*Saccharomyces* yeast species, naturally found in grape must, may affect wine quality positively or negatively. These yeasts are of growing interest in winemaking for shaping wine flavours of natural grape musts, and they are predominantly found in the earlier stages of wine fermentation (Ciani et al., 2010; Henschke and Jiranek, 1993; Jolly et al., 2003; Lane and Morrissey, 2010). They are typically outcompeted by *Saccharomyces cerevisiae* strains in the medium, mainly due to their low resistance to ethanol. The impacts of selected yeast species on wine properties have been largely described in literature. *Torulaspora delbrueckii*, produces polyols, low volatile acidity, and high succinate (Ballester-Tomás et al., 2017; Brandam et al., 2013; Ivit et al., 2020; Mbuyane et al., 2018; Tondini et al., 2020). *Starmerella bacillaris* shows variations in carbon metabolism including high glycerol yields and lows alcohol and acetate yields (Contreras et al., 2015; Englezos et al., 2018). *Metschnikowia pulcherrima* produces relevant higher alcohols and reduces ethanol concentration, particularly during mixed fermentation, and simultaneously favour the production of esters and higher alcohols such as phenylethanol (Contreras et al., 2015; Jolly et al., 2014; Morales et al., 2015; Quirós et al.,

2014; Sadineni et al., 2012). The inoculation of *Lachancea thermotolerans* typically results in wines with low volatile acidity and certain strains produce lactic acid, thereby increasing wine's titratable acidity (Bagheri et al., 2018; Binati et al., 2020; Ciani et al., 2010; Comitini et al., 2021; Jolly et al., 2014; Morata et al., 2018). Finally, *Kluyveromyces marxianus* produces higher concentrations of certain aroma compound from the Ehrlich pathway (Labuschagne et al., 2021; Rollero et al., 2019). These metabolic differences are likely connected to the genetic background of the yeasts (Ayer et al., 2012; Harrison et al., 2007; Henriques et al., 2021; Li and Bao, 2007; van Hoek and Merks, 2012a), especially their ability to catalyse certain reactions and to manage their intracellular redox balance. Nevertheless, limited knowledge is available regarding the strategies used by the non-*Saccharomyces* species to manage the NAD(H) and NADP(H) turnover and the subsequent consequences on the formation of central carbon metabolites and volatile compounds.

The aim of this study was to survey the landscape of redox status dynamics amongst yeast species throughout alcoholic fermentation under conditions simulating those of winemaking in order to better comprehend the differences observed in terms of fermentation performances and flavour production. We selected wine yeast species known for their varying fermentation abilities and response to available oxygen and sugars. Using a metabolomics approach, we assessed intracellular redox cofactors and extracellular by-products to determine the redox state of the different strains over time and correlate it with the yeast metabolic activity.

2. Materials and Methods

2.1. Yeast strains and growth conditions

2.1.1. Yeast Strains

The yeasts investigated were selected from a variety of wine yeast species known for possessing a range of fermentation performance abilities and differing response to the presence of oxygen and sugars (Crabtree effect). They were chosen from the natural isolates in the culture collections of the South African Grape and Wine Research Institute (SAGWRI; formerly Institute for Wine Biotechnology (IWBT), Stellenbosch University, South Africa), the Centre International de Ressources Microbiennes. (CIRM, France)), and Lallemand Inc. (Montreal, QC, Canada) (Table 1). They were cryopreserved at −80°C in 20% (v/v) glycerol Yeast Peptone Dextrose (YPD) medium (10 g/L yeast extract. 20 g/L peptone. 20 g/L glucose) and cultivated on YPD agar plate (YPD + 20 g/L agar).

Table 1

Cryopreserved yeast cultures were thawed at room temperature, and then streaked on YPD agar. Thereafter, a preculture was prepared for each yeast strain by inoculating a single colony into 50 mL of YPD broth, which was then incubated at 28°C under agitation at 180 rpm for 12 - 15 h. The

MultisizerTM 3 Coulter Counter (Beckman Coulter, Brea, CA, USA) was used to calculate the cell density of each strain. Thereafter, all strains were inoculated from their respective preculture at a cell density of 1×10^6 cells/mL.

2.1.2. Synthetic grape must medium

A synthetic grape must (SM) medium that mimics grape juice composition was used containing 200 g/L sugars (100 g/L glucose and 100 g/L fructose) (Table S1), and 200 mg/L yeast assimilable nitrogen (YAN) as a mixture of amino acids (Table S2) and ammonium, trace elements (Table S3), and vitamins (Table S4) as described by Bely et al. (1990). The pH of the medium was adjusted to 3.3 using 10 M NaOH.

2.1.3. Fermentation conditions

Triplicate fermentations were carried out in 330-mL glass flasks equipped with a sampling port containing 250 mL of SM medium for each strain. These flasks were also equipped with water-filled fermentation locks in order to maintain self-generated anaerobiosis during fermentation. Steam-pasteurisation of the flasks with SM was carried out at 100°C for 15 min to ensure asepsis without destroying thermolabile compounds such as vitamins. Then, the medium was saturated with sterile air for 20 min while being constantly agitated to balance the levels of dissolved and headspace oxygen. Furthermore, after sparging and before inoculation, under sterile conditions the SM was supplemented with 5 mg/L phytosterols in order to meet the lipid requirements of the yeast during anaerobic growth. The phytosterol stock solution, prepared with a commercial solution of β-sitosterol >70% (Sigma 85541) that also contains other sterols, was composed of 20 g/L β-sitosterol (Sigma-Aldrich, St. Louis, MO, USA), Tween 80 (Sigma-Aldrich)/absolute ethanol (1:1, v/v) in the stock solution. The medium was fermented under isothermal conditions at 22°C with continuous agitation at 250 rpm.

2.2. Analytical methods

2.2.1. Fermentation, growth kinetics, and cell dry biomass.

The progress of the fermentations was monitored by the release of CO_2 determined by measuring the weight of the fermentation flasks. For the initial three days of fermentation, the flasks were weighed at least five times daily, with measurements taken at 3-hour intervals. This approach was particularly useful for strains known for their high fermentation kinetics as it allowed for a clear depiction of the CO_2 production rate and the transition from the lag phase to the exponential phase. Several parameters of fermentation kinetics were calculated: the lag time, the maximum rate of fermentation (Rmax), the time to reach Rmax, the CO_2 produced at Rmax, the rate of fermentation when 30 and 60 g/L CO_2 was produced. With the exception of fermentation duration, all of these

parameters were extracted from the weight loss data using the in-house R package alfisStatUtilR (v1.0.0) based on a local regression and likelihood model that smooth the data with the locfit function (Loader, 2013). In this model, the rate of CO_2 production was calculated by polynomial smoothing of the last 10 fermenter weight measurements. The lag phase is defined as the period from the beginning of fermentation to the point at which 1 g/L cumulative CO_2 has been produced. The end of fermentation (EF) was defined as the time when CO_2 production rate reached stable values ≤ 0.02 g/L/h for a continuous period of 48 h.

Yeast growth was monitored by measuring the absorbance of the culture at 600 nm (OD600). The intracellular redox state was investigated at three points during fermentation based on the growth curve values and time of cultivation from preliminary fermentations. We used the following modified Gompertz function, previously described by Zwietering et al. (1990), on the growth curves data in order to determine the sampling points for each strain based on its physiological state during the fermentation.

Function to fit:

$$G(t) = Aexp\left\{-exp\left[\frac{\mu_{max} \times e}{A}(\lambda - t) + 1\right]\right\}$$

Where G(t) is the cell population at time t (in this study calculated as ln[OD600(t)/OD600(t_0)]), A is the maximum population level (Y units), μ_{max} the maximum growth rate (h^{-1}) and λ the lag time (h) defined as the time axis intercept of the tangent through the inflection point.

Therefore, intracellular redox state was determined from culture samples that were collected at mid-growth phase at 50% OD (corresponding to entry into exponential CO_2 production), maximum population (corresponding to entry into stationary growth phase and with a CO_2 concentration of 30 g/L for some strains), and at mid-stationary growth phase with a CO_2 concentration of 60 g/L.

Dry biomass was determined by filtering 10 mL of culture through a 0.45-µm pore size nitrocellulose filter (Millipore®). The filter was then rinsed twice with 50 mL of distilled water and dried in an oven at 110°C for 48 h (until no more weight loss was observed).

2.2.2. Quenching and quantification of redox cofactors

The concentration of redox cofactors was determined from a population of 10^7 cells for each cofactor pair. At different stages of fermentation, the yeast cellular metabolism was instantly inactivated (quenched) using a HEPES/methanol mixture (Faijes et al., 2007). Briefly, a 1 mL culture sample was transferred to a pre-chilled tube containing a cold (-80°C) mixture of HEPES/methanol (60% methanol in 10 mM HEPES buffer at pH 7.1). The cells and the supernatant were separated using a pre-chilled (-

10°C) centrifuge at 5000 rpm for five minutes. Then, the obtained pellets were frozen at -80°C until NAD(H) and NADP(H) were extracted. The cofactors were extracted and quantified according to the supplier's protocols, NAD(H) (MAK037) and (MAK038) (Sigma-Aldrich). At each sampling point, the biomass was used to normalize the redox cofactor concentrations.

2.2.3. Quantification of primary metabolites

The concentrations of yeast primary metabolites such as ethanol, glycerol, acetate, α-ketoglutarate, and succinate were determined by HPLC (HPLC 1260 Infinity, Agilent™ Technologies, Santa Clara, CA, USA) on a Phenomenex Rezex ROA column (Phenomenex™, Le Pecq, France) at 60 °C. The column was eluted with 0.005 N H_2SO_4 at a flow rate of 0.6 mL/min. Organic acids with the exception of succinate were analyzed with a UV detector (Agilent Technologies) at 210 nm; the concentrations of the other compounds including succinate were quantified with a refractive index detector (Agilent Technologies). Analysis was carried out with the Agilent™ OpenLab CDS 2. x software package.

2.2.4. Quantification of selected secondary metabolites

The concentrations of ethyl acetate, ethyl propanoate, ethyl 2-methylpropanoate, ethyl butanoate, ethyl 2-methylbutanoate, ethyl 3-methylbutanoate, ethyl hexanoate, ethyl octanoate, ethyl decanoate, ethyl dodecanoate, ethyl lactate, diethyl succinate, 2-methylpropyl acetate, 2-methylbutyl acetate, 3-methyl butyl acetate, 2-phenylethyl acetate, 2-methylpropanol, 2-methylbutanol, 3-methylbutanol, hexanol, 2-phenylethanol, propanoic acid, butanoic acid, 2-methylpropanoic acid, 2-methylbutanoic acid, 3-methylbutanoic acid, hexanoic acid, octanoic acid, decanoic acid, and dodecanoic acid were measured in the liquid phase after sample pre-treatment by double liquid-liquid extraction with dichloromethane in the presence of deuterated standards (Rollero et al., 2015). Samples were analyzed with an Agilent 8860 gas chromatograph (Agilent Technologies) equipped with an Agilent 7693A Autosampler (Agilent Technologies and coupled to an Agilent 5977B mass spectrometer (Agilent TechnologiesData were acquired and processed on OpenLab CDS 2 software (Agilent Technologies, Santa Clara, California, USA). The gas chromatograph was fitted with a ZB-WAX 30 m×0.25 mm×0.25 µm fused silica capillary column (Phenomenex). Helium was used as carrier gas (Air Products, Allentown, Pennsylvania, USA) at a constant flow rate of 1 mL/min. The following oven parameters were used for this analysis: initial temperature was 40°C held for 3 min, followed by an increase at a rate of 4°C/min to 160°C , then an increase at a rate of 15°C/min until 220°C and finally an increase at a rate of 20°C/min until 240°C held at this temperature for 10 min. Injector was set at 240°C, the autosampler was tempered to 8°C and sample volume was 2 µL injected in split mode at a split ratio of 10:1. The mass spectrometer quadrupole temperature was set at 150°C, the ion source was set at 230°C, and the transfer line at 240°C. For

quantification, mass spectra were acquired in Selected Ion Monitoring (SIM) mode at an electron impact energy of 70 eV.

2.2.5. Quantification of acetoin and 2.3-butanediol

Acetoin and 2,3-butanediol were analyzed by GC-FID after a double liquid-liquid extraction in chloroform in the presence of 1 mL internal standard (hexanol, 1:1000 v/v). The organic phase was dried and injected into the GC column. The apparatus used includes a HP 5890 gas chromatograph (Agilent Technologies) equipped with an SGE™ BP20 polar column (30 m x 0.53 mm x 1.0 µm) and coupled to a flame ionization detector.

2.3. Statistical analyses

All the experiments were carried out in biological triplicates. Statistical analyses were performed with R version 4.2.3 (The R Foundation for statistical computing, 2023). The aov function in R was used to implement one-way and two-way ANOVA, and when p-values were less than 0.05, the post-hoc Tukey's honesty significance difference (HSD) test, which is performed with the agricolae package (v1.3.5), was used to assess significant differences between the means. XLSTAT version 2023.1.1 (Addinsoft, NY, USA) was used for the Principal Component Analysis (PCA) of the secondary metabolites.

3. Results

We conducted fermentations in conditions mimicking those of wine fermentation in order to survey the landscape of intracellular redox status and compare the dynamics of the redox metabolism in eight individual strains from different wine yeast species (Table 1) throughout alcoholic fermentation. Alcoholic fermentations were monitored until no more weight loss was recorded. NAD(H) and NADP(H) concentrations were quantified at mid-exponential growth phase and when 30 g/L and 60 g/L CO_2 had been released, except for SbMTF3768, SbMTF3800, and Mp1 which did not reach 60 g/L CO_2 release. These time points were determined in preliminary fermentations (data not shown). At the same time points, the concentrations of yeast primary metabolites and dry biomass were quantified. The concentrations of the main secondary metabolites (i.e. major flavour compounds) were determined at the end of fermentation.

3.1. Wine yeast synthetic grape juice fermentation kinetics.

The comparison of key fermentation parameters from kinetics curves (Fig. 1, Table 2, Fig. S1) revealed important differences between strains in their fermentation capacity.

As expected, Sc1 exhibited the highest fermentation performances, completed fermentation in the shortest time (265 h) with the highest fermentation rates (Rmax: 1.0 g/L/h, rate at 30 g/L CO_2: 0.95

g/L/h, rate at 60 g/L CO_2: 0.75 g/L/h) and a short lag time (13 h). On the contrary, the non-*Saccharomyces* yeast strains exhibited slower fermentation kinetics, and their major fermentation parameters differed significantly. We noticed strain variations regarding their fermentation kinetics, even among strains of the same species, however, intra-specific similarities were also observed.

Td1, LtY1240, and Lt1 exhibited an intermediate level of fermentative capacity. These yeasts displayed the ability to consume most of the sugars (production of $C0_2$ of 94, 93.1, and 83.8 g/L, respectively) and reached the end of fermentation within a reasonable timeframe (374, 433, and 374 h, respectively). This longer fermentation time compared to *S. cerevisiae* is explained by lower fermentation rates throughout the process, and in particular during the stationary phase, with between 1.8- (Td1) and 2.7- (LtY1240, and Lt1) times lower rates at 60 g/L of CO_2 (Table2).

On the other hand, KmY885, SbMTF3768, SbMT3800, and Mp1 demonstrated a lower capacity for fermentation, with species-dependent characteristics. First, KmY885 displayed a notable ability to carry out virtually complete fermentation producing 85 g/L CO_2. However, the consumption of sugar by this strain was achieved over an extended period compared to all other yeasts, of 808 h. In fact, KmY885 showed a longer lag time than the other strains (56 h), combined with a low fermentation rate from the beginning of fermentation (Rmax: 0.21 g/L/h), but an ability to maintain this fermentative activity for an extended period of time (Fig. 1). SbMTF3768, SbMT3800, and Mp1 were unable to complete the fermentation and ceased to ferment after having released 51.7, 52.5 and 42.7 g/L of CO_2 at the end of fermentation, respectively. The two *Starmerella bacillaris* strains had similar fermentation profiles, characterised by a lag phase of around 30 h, followed by a gradual increase in fermentation rate over 60 h to reach a maximum level of 0.33 g/L/h. In contrast, Mp1 differentiated by the shortest lag phase (10 h), but by a low fermentative activity. The rate of fermentation, displaying a maximum value of 0.25 g/L/h, suddenly dropped sharply after 31 h of fermentation.

Interestingly, the formation of biomass of strains with good or intermediate fermentation performances, ranging from 3.0 to 3.8 g/L was higher than that of strains with low fermentation capacities, varying between 1.1 and 1.7 g/L (Table 3).

3.2. Quantification of NAD(H) and NADP(H) cofactors during synthetic grape must fermentation

Total concentration of NAD(H) and NADP(H) and those of their respective forms (i.e., oxidised and reduced) in yeast pellets were measured at 3 different stages of fermentation (mid-exponential growth phase and when 30 g/L and 60 g/L CO_2 had been released). By focusing on these specific time points, we aimed to capture major changes in the yeast metabolism and obtain a clearer understanding of cofactor dynamics during fermentation. Overall, while the NAD^+/NAD(H) pair underwent significant changes during fermentation depending on the strains, the $NADP^+$/NADP(H) pair tended to maintain a relative balance with only minor fluctuations in both the ratio and total concentration (Fig. 2). Additionally, the total NADP(H) concentration within the cells was considerably lower across all strains compared to total NAD(H) levels.

Regarding NADP(H) levels (Fig. 2A), there were no marked differences observed between strains during fermentation. The total pool for this cofactor ranged between 12 and 27 pmol per 10^7 cells, with only small variations amongst strains. With the exception of SbMTF3800 and Mp1, the levels of total NADP(H) tended to increase between 50% OD, as the strain entered into exponential CO_2 production, and 30 g/L CO_2. Overall, the ratio of $NADP^+$/NADPH remained unchanged throughout the fermentation, remaining between 0.68 and 1.09, with some exceptions. Some yeast strains (Lt1, KmY885 and SbMTF3800) displayed a redox state that slightly favoured NADPH during the growth stage, but the balance was restored as the fermentation progressed.

In contrast, a high variability in the concentration of total NAD(H) was observed depending on both the species and the fermentation stage (Fig 2B). At 50% population, NAD(H) concentration was above 100 pmol/10^6 cells for strains with the highest fermentation performance, Sc1, Td1, and LtY1240. Their intracellular NAD(H) concentrations remained high until 30 g/L of CO_2 had been released, before dropping drastically. Strains with lower fermentative capacity exhibited lower NAD(H) concentrations at the beginning of fermentation compared to Sc1, Td1, and LtY1240, below 80 pmol/10^6 cells. In addition, for strains able to produce at least 60 g/L CO_2 despite their low fermentation performances (KmY885 and Lt1), total intracellular NAD(H) also consistently declined during the last part of fermentation. A notable variation amongst species was observed in the NAD^+/NADH ratio, which is a good indicator of the balance between the reduced and oxidised forms of this cofactor. The ratio measured in *L. thermotolerans* was in general lower than that of Sc1 and Td1, due to the limited amount of NAD^+ in this former species. Interestingly, KmY885 was the only strain for which the NAD^+/NADH ratio remained high after production of 30 or 60 g/L of CO_2. All these species managed to maintain NAD^+ concentration above 10 mmol/10^6 cells throughout the

fermentation. Regarding SbMTF3768, SbMTF3800, and Mp1, by the time the CO_2 reached 30 g/L, NAD^+ approached depletion with concentrations lower than 2 pmol/10^6 cells and ratios close to zero.

In summary, all strains eventually reached a reduced state, with a pool of NAD(H) in favour of NADH over NAD^+, with varying degrees of reduction observed amongst them. Some strains displayed only slight reduction (Sc1, Td1, LtY1240, and KmY885), while others exhibited more pronounced degree of reduction (Lt1, SbMTF3768, SbMTF3800, and Mp1).

3.3. Primary metabolites production between yeasts as impacted by redox balance requirements.

Variations were observed in the production of primary metabolites amongst the different yeast strains (Table 4), including ethanol, glycerol, acetate, succinate, and lactate. As sugar consumption significantly varied depending on the strains (Table 4), we compared the yields of production of central carbon metabolites ($mM_{metabolite}$ per M of sugars consumed) to better understand their specificities regarding the partitioning of carbon fluxes within the metabolic network and their redox balance mechanisms (Fig. 3).

First, significant differences were found in the yield of production of ethanol. Sc1 exhibited the highest yield (1849 mM/M) while KmY885, which displayed intermediate fermentation behaviour, had the lowest ethanol yield (1749 mM/M). Interestingly, the ethanol yield in Td1 was comparable to that of Lt1 (1818 mM/M and 1812 mM/M respectively), while LtY1240 had a higher yield than these two strains (1838.52 mM/M). Finally, strains with the weakest fermentative behaviour (Mp1, SbMTF3768 and SbMTF3800) showed a low ethanol yield (1796 mM/M, 1764 mM/M and 1768 mM/M respectively).

Beyond ethanol, glycerol production differed between strains (Table 3 and Table S6). Non-*Saccharomyces* yeasts exhibited higher levels of glycerol yields compared to *S. cerevisiae* (60 mM/M). Interestingly, the yeasts with the lowest fermentation capacities, SbMTF3800, SbMTF3768, and Mp1 displayed the highest yields of glycerol production (144 mM/M, 137 mM/M, and 116 mM/M, respectively). KmY885 produced the highest amount of glycerol, 9.8 g/L. This species also differentiated by its high production of acetate, of 1.95 g/L corresponding to a yield of 35 mM/M. This yield is the highest among all strains, including S. cerevisiae (7.9 mM/M). The other non-*Saccharomyces* species exhibited yields of production of acetate lower than that of *S. cerevisiae*, in particular Td1 (1.5 mM/M). It is noteworthy that in KmY885, glycerol and acetate were continuously produced throughout fermentation, while they were mainly synthetised during the growth phase (up to 30 g/L CO_2) by the other strains (Fig. S1 E and Table S6).

Td1 differed from the other species directing a substantial part of glucose towards the formation of succinate (15.6 mM/M), resulting in a final production of 2.1 g/L (Table 3, Table S6, and Fig S1 B). Lt1 was the only yeast to produce large amounts of lactate, with yield of production of 44.7 mM/M. Surprisingly, the formation of lactate by the second *L. thermotolerans* strain LtY1240 was low, with a yield of production of 1.5 mM/M, similar to that of *S. cerevisiae* (1.8 mM/M). An important variability was observed between strains in their capacity to produce 2,3-butanediol: Lt1 and Mp1 did not produce this compound, while the other species produced 2,3-butanediol, with a yield of production ranging from 0.16 to 3.7 mM/M. Finally, all the strains displayed a low capacity to produce acetoin, only detected as traces at the end of fermentation conducted with Lt1, SbMTF3768 and SbMTF3800.

3.4. Production of secondary metabolites by the different yeasts

To provide an overview of the production of major aroma compounds (secondary metabolites) at the end of fermentation by the different yeast strains, we used a principal component analysis (PCA) biplot to show the product yields of the aroma compounds grouped according to their metabolic origin (Fig 4). Fusel alcohols and acids and their ester derivatives were grouped according to alpha-keto acid intermediates of the Ehrlich pathway that they derive from. In addition, medium chain fatty acids and their ethyl esters were grouped together as they derived from acetyl-CoA.

The data reveal notable differences in the production of secondary metabolites amongst yeast species, with strains from the same species exhibiting similar profiles (Fig 4). Sc1 differed from the rest of the strains by demonstrating the highest product yields of α-keto-γ-(methylthio)butyrate (αKMBA) (catabolism of methionine), α-ketoisocaproate (catabolism of leucine), and α-ketomethylvalerate (cababolism of isoleucine) derivatives. This strain also positively correlated with a large production of short-/medium-chain fatty acids (S/MCFAs) and ethyl esters associated with these metabolites. Td1 exhibited a similar profile of formation of volatile compounds, but with lower yields. The strain Mp1 was characterized by high level of α-ketoisovalerate and phenylpyruvate derivatives, combined with a low capacity to produce the other volatile compounds. The capacity to produce ethyl lactate and derivatives of α-ketobutyrate separated *L. thermotolerans* strains – in particular Lt1- from the other species. Finally, *S. bacillaris* strains showed intermediate abilities for the production of ethyl lactate, α-ketoisovalerate and α-ketobutyrate derivatives.

Beyond this overall picture, analysis of the production of each volatile compound has enabled us to go further in characterising the metabolic specificities of each strain. The Td1 strain produced higher alcohols amounts comparable to those produced by Sc1, but stood out for its very limited capacity to produce acetate esters. The yield of conversion of higher alcohols to acetate esters was 10 times lower in Td1 than in Sc1. More generally, non-*Saccharomyces* yeasts were low producers of acetate

esters with the exception of KmY885, which had a 4 times higher capacity to produce acetate esters than Sc1. Interestingly, strains associated with low fermentative performances produced high levels of isobutanol: 245.8 mg/L, 130.0 mg/L, and 192.5 mg/L by Mp1, SbMTF3768 and SbMTF3800, respectively (Table 4). Conversely, the strong fermenters Sc1, Td1, Lt1, and LtY1240 promoted the formation of isoamyl alcohol, with concentrations of 395.96 mg/L, 334.6 mg/L, 380.91 mg/L, 317.7mg/L, respectively. In addition, the two *L. thermotolerans* strains Lt1 and LtY1240 were the highest producers of propanol, with concentrations of 56.1 mg/L and 59.2 mg/L, respectively. Finally, the high capacity of Mp1 to synthesise higher alcohols despite its low capacity to consume sugars, must be mentioned. As an example, this strain synthetized an amount of phenylethanol similar to that of Sc1 while consuming half as much sugar. Overall, the production of secondary metabolites by different yeasts varied considerably between species and, to a lesser extent, between strains of the same species.

4. Discussion

The balance between reduced and oxidised redox factors is a physiological requirement with huge implications on the profile of metabolites produced from sugars by *S. cerevisiae* during fermentation. This is primarily because the redox balance is maintained exclusively by the central metabolism, which depends on the genetic background of the yeast strain but also adapts to changes in the environment, such as nutrient availability. Consequently, various compounds are synthetized as redox sinks including glycerol and organic acids (acetate, pyruvate, succinate) (Bakker et al., 2001; Croft et al., 2020; Sáez and Lagunas, 1976; van Dijken and Scheffers, 1986). Furthermore, the intracellular NAD(P)(H) content modulates the formation of a wide range of molecules, including volatile compounds (Bloem et al., 2016; Celton et al., 2012a, 2012b). The present study aimed to explore the variability of redox status within wine yeast species over fermentation. In particular, we wanted to know whether the availability of cofactors differed depending on the species and to elucidate the further consequences on their fermentation performances and production of metabolites.

It has recently been established that during anaerobic wine fermentation, the two major couples of redox cofactors in *S. cerevisiae* display different dynamics (Duncan et al., 2023). While NADP(H) level and ratio were stable, intracellular NAD(H) levels decreased during fermentation, that deviates from the generally accepted view of a redox cofactor pool at a constant level (Bakker et al., 2001; de Koning and van Dam, 1992; Richard et al., 1993; Sáez and Lagunas, 1976). In this study, monitoring the redox status changes of 8 wine yeasts revealed that this global drop in NAD(H) levels also applies to other yeasts such as *L. thermotolerans*, *T. delbrueckii* and *K. marxianus* species, exhibiting NAD(H) levels after production of 60 g/L of CO_2 at least two-times lower than at the beginning of

fermentation. Additionally, we found that the intracellular availability of both NAD^+ and NADH had a distinctive profile throughout the fermentation according to the strain and these changes in the redox status dynamics could explain the respective fermentation kinetics and performance of the species. Sc1, Td1, Lt1 and LtY1240 were characterised by a high content of NAD(H) during the two first stages of fermentation (97 pmol/10^6 cells on average, compared to 72 pmol/10^6 cells for the other strains) combined with a ratio NAD^+/NADH favouring NADH throughout the fermentation. However, these strains displayed a substantial level of NAD^+, above 13 pmol/10^6 cells, when 60 g/L CO_2 was released, showing their capacity to manage the redox balance all along the fermentation. Interestingly, these 4 strains showed the best growth capacity and fermentation performances. Conversely, Mp1, SbMF3800 and SbMTF3768, in addition to their lower levels of NAD(H), were associated with a depletion of the oxidised cofactor NAD^+ observed as soon as 30 g/L of CO_2 was produced (concentrations ranging from not detectable to 3 pmol/10^6 cells). These yeasts displayed poor growth and have proved unable to complete fermentation. Finally, *K. marxianus* KmY885 stood out for its capacity to balance the availability in reduced and oxidised cofactors (NAD^+/NADH ratio around 0.9), despite a low NAD(H) intracellular concentration. This strain, even with a weak growth, consumed most of the sugars at a low but constant rate. Overall, our observations reveal that a limited ability to regenerate oxidised cofactor NAD^+ contributes, at least in part, to the poor growth and fermentation capacities of some wine yeast species.

The formation of glycerol has been widely described as the main pathway for the regeneration of NAD^+ from NADH, synthesised in excess for the formation of biomass (Ansell et al., 1997; Bakker et al., 2001; Larsson et al., 1998; Pronk et al., 1996). Additionally, the formation of 2,3-butanediol and, to a lesser extent, succinate through the TCA reductive pathway can also act as valuable NADH redox valves (Camarasa et al., 2003; Ehsani et al., 2009). Interestingly, the yield of glycerol formation with respect to the sugar consumed by the different strains studied varied substantially and inversely with their growth and fermentation capacity, comprised between 59 mM/M for Sc1 and 140 mM/M for *S. bacillaris* strains (Fig S2). Increased flux in the glycerol pathway is sufficient to cover the increased demand for NAD^+ in Td1, Lt1, LtY1240, and KmY885. Conversely, in Mp1, SbMTF3768, and SbMTF3800, the flux of conversion of glucose to glycerol (and to a lesser extent, 2,3-butanediol and succinate) is insufficient to maintain redox balance, despite a greater proportion of glucose being used in these metabolic pathways. This disparity in metabolic pathways within *S. cerevisiae* may be one of the origins of the limited fermentative activity and fermentation issues observed in these strains.

Differences in the flux partitioning of the carbon network among yeasts are further by the strain-dependent yields of production for the other compounds. 2,3-butanediol production remains notably

low (below 8.8 mM/M), with LtY1240 yielding the highest at 3.7 mM/M. In contrast, KmY885, Lt1, Mp1, and Td1 preferentially favour succinate production, with yields ranging from 10.6 to 15.6 mM/M. These observations reveal the key role of the formation of glycerol in the management of redox balance for all the studied yeast species. Furthermore, they display specific redox requirements for growth and fermentation (Albers et al., 1998, 1996) and exploit the plasticity of yeasts genome (Ambroset et al., 2011; Legras et al., 2018; Marsit and Dequin, 2015) and gene interactions (Harrison et al., 2007) in order to adapt to the grape juice environment during the fermentation process.

Lactic acid production in *L. thermotolerans* strains shows significant variation (Banilas et al., 2016; Hranilovic et al., 2018; Vicente et al., 2023), possibly due to repression in some strains (Battjes et al., 2023) and up-regulation (Shekhawat et al., 2020) one or more the LDH genes. Oxygen availability also appear to influence *L. thermotolerans* strains' persistence in wine, and consequently lactate production by (Shekawat et al. 2019; Battjes et al 2023). When comparing the carbon balances of Sc1 with low (LtY1240) and high (Lt1) lactate producers, we observed that Lt1 replaces a portion of ethanol or lactate production, possibly due to its higher LDH activity compared to other yeast strains. However, this substitution does not significantly alter the redox balance. This can be explained by the fact that, from a redox perspective, the conversion of pyruvate into ethanol and/or lactate is essentially equivalent, involving the oxidation of 1 mole NADH/mol.

The regeneration of NADPH, which is consumed during anabolic reactions, occurs through two primary pathways in *S cerevisiae*: the pentose phosphate pathway (involving enzymes Zwf1p and Gnd1p), and the oxidation of acetaldehyde to acetate, catalysed by NADP-dependent acetaldehyde dehydrogenases Ald6p and Ald4p (Bruinenberg et al., 1983; Celton et al., 2012a; Grabowska and Chelstowska, 2003; Remize et al., 2000; Saint-Prix et al., 2004). Although $NADP^+$ and NADPH concentrations, as well as their ratios, remain similar regardless of the yeast strain or fermentation stage, consistent with prior research (Cadière et al., 2011; Duncan et al., 2023), we have observed significant variability in acetate production among the strains (Fig. 4 and Fig. S2).
Different hypotheses can be suggested to explain these observations. First, low acetate yields can be attributed to an increased conversion of acetate to acetyl-CoA, driven by the demand for lipid biosynthesis as shown by Cadière et al. (2010) in an evolved strain of *S. cerevisiae*. In light of this, a similar phenomenon could explain the decrease in acetate yields in non-*Saccharomyces* yeasts, suggesting a minor role of acetate production for the management of NADP(H) in these yeasts. Secondly, the observed increase in acetate production, e.g., in KmY885, may reflect a fine-tuning

strategy for the production of NADP(H) and metabolic processes to meet anabolic demands, thereby resulting in a stable intracellular cofactor pools.

Finally, we were interested in whether the redox status of the different yeast species had an impact on the formation of volatile compounds. The main classes of fermentative aromas include fusel alcohols acids, acetate esters, medium chain fatty acids and ethyl esters. In yeast, the production of fusel alcohols and acids and their corresponding ester derivatives is achieved by the catabolism of alpha-keto acids. Alpha-keto acids may be produced by transamination of the assimilated amino acids (Hazelwood et al., 2008), alternatively they may be *de novo* produced through central carbon network (Crépin et al., 2017; Rollero et al., 2019). The synthesis of MCFAs consists of two-carbon-unit elongations of the carbon chain, using acetyl-CoA. It appears that the synthesis of all these molecules involves a wide range of dehydrogenases (Hazelwood et al., 2008; Lilly et al., 2006) and it has been previously shown that the modulation of cofactor demand has an impact on their formation in *S. cerevisiae* (Bloem et al., 2016; Celton et al., 2012a).

Interestingly, the strains showing a high degree of reduction (high NADH/NAD^+ ratio combined with low fermentative capacity) favoured the production of higher alcohols at the expense of the corresponding fusel acids in the respective pathways. This is in line with the low NAD^+ availability in these yeasts. Furthermore, we found that *M. pulcherrima* and *S. bacillaris* strains produced low level of MCFAs and acetate esters and accumulated high levels of isobutanol at the expense of isoamyl alcohol. This profile of volatile compounds production likely reflects the low capacity of these yeasts to produce oxidised compounds, in particular acetate. Indeed, acetate is the precursor of acetyl-CoA involved in MCFAs and acetate esters formation and is also required, together with NAD^+, for the conversion of α-ketoisovalerate (precursor of isobutanol) to α-ketoisocaproate (precursor of isoamyl alcohol)(Rollero et al., 2019). Supporting this pattern, KmY885, as the strain with balanced levels of NAD^+ and NADH throughout the fermentation, was able to synthetize oxidised compounds and produced high levels of isoamyl alcohol and displayed a high yield of conversion of fusel alcohols to acetate esters compared *S. cerevisiae.*

Overall, our observations demonstrate that redox status of the yeasts may directly modulate the formation of volatile or indirectly, through the formation of precursors.

In conclusion, the redox state of a yeast cell is therefore an important factor that can influence its fermentation performance and metabolite production. This study demonstrates that yeast strains employ diverse approaches to maintain redox balance, which may have implications for their metabolic activities and the production of various compounds during fermentation. By understanding the mechanisms by which yeast cells manage their intracellular redox state, it is

possible to improve the fermentation performance during wine production and ultimately the metabolic footprint of the different yeast species/strains.

5. Funding

This study was supported by Stellenbosch University (Stellenbosch, South Africa), the Organisation Internationale de la Vigne et du Vin (Paris, France), The Embassy of France in South Africa, Winetech (Paarl, South Africa) (Winetech project number NP10.2020) and Lallemand Oenology (Blagnac, France).

6. Declaration of competing interest

The authors state that they have no financial conflicts of interest or personal relationships that could have influenced the work reported in this paper.

7. Acknowledgments

We thank Pascale Fernandez-Valle, Faïza Macna, Teddy Godet, Marc Perez, and Christian Picou for their technical assistance.

8. References

Albers, E., Larsson, C., Lidén, G., Niklasson, C., Gustafsson, L., 1996. Influence of the nitrogen source on *Saccharomyces cerevisiae* anaerobic growth and product formation. Appl. Environ. Microbiol. 62, 3187–3195. https://doi.org/10.1128/aem.62.9.3187-3195.1996

Albers, E., Lidén, G., Larsson, C., Gustafsson, L., 1998. Anaerobic redox balance and nitrogen metabolism in *Saccharomyces cerevisiae*. Recent Dev. Microbiol. 2, 253–279.

Ambroset, C., Petit, M., Brion, C., Sanchez, I., Delobel, P., Guérin, C., Chiapello, H., Nicolas, P., Bigey, F., Dequin, S., Blondin, B., 2011. Deciphering the Molecular Basis of Wine Yeast Fermentation Traits Using a Combined Genetic and Genomic Approach. G3 Genes|Genomes|Genetics 1, 263–281. https://doi.org/10.1534/g3.111.000422

Anderson, R.G., 1989. Yeast and the victorian brewers: incidents and personalities in the search for the true ferment. J. Inst. Brew. 95, 337–345. https://doi.org/10.1002/j.2050-0416.1989.tb04641.x

Ansell, R., Granath, K., Hohmann, S., Thevelein, J.M., Adler, L., 1997. The two isoenzymes for yeast NAD^+ -dependent glycerol 3-phosphate dehydrogenase encoded by GPD1 and GPD2 have distinct roles in osmoadaptation and redox regulation. EMBO J. 16, 2179–2187. https://doi.org/10.1093/emboj/16.9.2179

Ayer, A., Fellermeier, S., Fife, C., Li, S.S., Smits, G., Meyer, A.J., Dawes, I.W., Perrone, G.G., 2012. A genome-wide screen in yeast identifies specific oxidative stress genes required for the maintenance of sub-cellular redox homeostasis. PLoS One 7, e44278. https://doi.org/10.1371/journal.pone.0044278

Bagheri, B., Zambelli, P., Vigentini, I., Bauer, F.F., Setati, M.E., 2018. Investigating the effect of selected non-*Saccharomyces* species on wine ecosystem function and major volatiles. Front. Bioeng. Biotechnol. 6, 1–12. https://doi.org/10.3389/fbioe.2018.00169

Bakker, B.M., Overkamp, K.M., van Maris, A.J.A., Kötter, P., Luttik, M.A.H., van Dijken, J.P., Pronk, J.T., 2001. Stoichiometry and compartmentation of NADH metabolism in *Saccharomyces cerevisiae*. FEMS Microbiol. Rev. 25, 15–37. https://doi.org/10.1111/j.1574-6976.2001.tb00570.x

Ballester-Tomás, L., Prieto, J.A., Gil, J. V., Baeza, M., Randez-Gil, F., 2017. The Antarctic yeast *Candida sake*: Understanding cold metabolism impact on wine. Int. J. Food Microbiol. 245, 59–65. https://doi.org/10.1016/j.ijfoodmicro.2017.01.009

Banilas, G., Sgouros, G., Nisiotou, A., 2016. Development of microsatellite markers for *Lachancea thermotolerans* typing and population structure of wine-associated isolates. Microbiol. Res. 193, 1–10. https://doi.org/10.1016/j.micres.2016.08.010

Barrajón-Simancas, N., Giese, E., Arévalo-Villena, M., Úbeda, J., Briones, A., 2011. Amino acid uptake by wild and commercial yeasts in single fermentations and co-fermentations. Food Chem. 127, 441–446. https://doi.org/10.1016/j.foodchem.2010.12.151

Battjes, J., Melkonian, C., Mendoza, S.N., Haver, A., Al-Nakeeb, K., Koza, A., Schrubbers, L., Wagner, M., Zeidan, A.A., Molenaar, D., Teusink, B., 2023. Ethanol-lactate transition of *Lachancea thermotolerans* is linked to nitrogen metabolism. Food Microbiol. 110, 104167. https://doi.org/10.1016/j.fm.2022.104167

Bely, M., Sablayrolles, J.-M., Barre, P., 1990. Automatic detection of assimilable nitrogen deficiencies during alcoholic fermentation in oenological conditions. J. Ferment. Bioeng. 70, 246–252. https://doi.org/10.1016/0922-338X(90)90057-4

Binati, R.L., Lemos Junior, W.J.F., Luzzini, G., Slaghenaufi, D., Ugliano, M., Torriani, S., 2020.

Contribution of non-*Saccharomyces* yeasts to wine volatile and sensory diversity: A study on *Lachancea thermotolerans*, *Metschnikowia* spp. and *Starmerella bacillaris* strains isolated in Italy. Int. J. Food Microbiol. 318, 108470. https://doi.org/10.1016/j.ijfoodmicro.2019.108470

Bloem, A., Sanchez, I., Dequin, S., Camarasa, C., 2016. Metabolic impact of redox cofactor perturbations on the formation of aroma compounds in *Saccharomyces cerevisiae*. Appl. Environ. Microbiol. 82, 174–183. https://doi.org/10.1128/AEM.02429-15

Brandam, C., Lai, Q.P., Julien-Ortiz, A., Taillandier, P., 2013. Influence of oxygen on alcoholic fermentation by a wine strain of *Torulaspora delbrueckii*: Kinetics and carbon mass balance. Biosci. Biotechnol. Biochem. 77, 1848–1853. https://doi.org/10.1271/bbb.130228

Bruinenberg, P.M., Van Dijken, J.P., Scheffers, W.A., 1983. A theoretical analysis of NADPH production and consumption in yeasts. J. Gen. Microbiol. 129, 953–964. https://doi.org/10.1099/00221287-129-4-953

Cadière, A., Galeote, V., Dequin, S., 2010. The *Saccharomyces cerevisiae* zinc factor protein Stb5p is required as a basal regulator of the pentose phosphate pathway. FEMS Yeast Res. 10, 819–827. https://doi.org/10.1111/j.1567-1364.2010.00672.x

Cadière, A., Ortiz-Julien, A., Camarasa, C., Dequin, S., 2011. Evolutionary engineered *Saccharomyces cerevisiae* wine yeast strains with increased in vivo flux through the pentose phosphate pathway. Metab. Eng. 13, 263–271. https://doi.org/10.1016/j.ymben.2011.01.008

Camarasa, C., Grivet, J.P., Dequin, S., 2003. Investigation by ^{13}C-NMR and tricarboxylic acid (TCA) deletion mutant analysis of pathways of succinate formation in *Saccharomyces cerevisiae* during anaerobic fermentation. Microbiology 149, 2669–2678. https://doi.org/10.1099/mic.0.26007-0

Carrau, F., Medina, K., Fariña, L., Boido, E., Dellacassa, E., 2010. Effect of *Saccharomyces cerevisiae* inoculum size on wine fermentation aroma compounds and its relation with assimilable nitrogen content. Int. J. Food Microbiol. 143, 81–85. https://doi.org/10.1016/j.ijfoodmicro.2010.07.024

Carrau, F.M., Medina, K., Farina, L., Boido, E., Henschke, P.A., Dellacassa, E., 2008. Production of fermentation aroma compounds by *Saccharomyces cerevisiae* wine yeasts: Effects of yeast assimilable nitrogen on two model strains. FEMS Yeast Res. 8, 1196–1207. https://doi.org/10.1111/j.1567-1364.2008.00412.x

Celton, M., Goelzer, A., Camarasa, C., Fromion, V., Dequin, S., 2012a. A constraint-based model analysis of the metabolic consequences of increased NADPH oxidation in *Saccharomyces cerevisiae*. Metab. Eng. 14, 366–379. https://doi.org/10.1016/j.ymben.2012.03.008

Celton, M., Sanchez, I., Goelzer, A., Fromion, V., Camarasa, C., Dequin, S., 2012b. A comparative transcriptomic, fluxomic and metabolomic analysis of the response of *Saccharomyces cerevisiae* to increases in NADPH oxidation. BMC Genomics 13, 1. https://doi.org/10.1186/1471-2164-13-317

Ciani, M., Comitini, F., Mannazzu, I., Domizio, P., 2010. Controlled mixed culture fermentation: A new perspective on the use of non-*Saccharomyces* yeasts in winemaking. FEMS Yeast Res. 10, 123–133. https://doi.org/10.1111/j.1567-1364.2009.00579.x

Comitini, F., Agarbati, A., Canonico, L., Ciani, M., 2021. Yeast interactions and molecular mechanisms in wine fermentation: A comprehensive review. Int. J. Mol. Sci. 22. https://doi.org/10.3390/ijms22147754

Contreras, A., Curtin, C., Varela, C., 2015. Yeast population dynamics reveal a potential 'collaboration'

between *Metschnikowia pulcherrima* and *Saccharomyces uvarum* for the production of reduced alcohol wines during Shiraz fermentation. Appl. Microbiol. Biotechnol. 99, 1885–1895. https://doi.org/10.1007/s00253-014-6193-6

Cortassa, S., Aon, J.C., Aon, M.A., 1995. Fluxes of carbon, phosphorylation, and redox intermediates during growth of *Saccharomyces cerevisiae* on different carbon sources. Biotechnol. Bioeng. 47, 193–208. https://doi.org/10.1002/bit.260470211

Crépin, L., Truong, N.M., Bloem, A., Sanchez, I., Dequin, S., Camarasa, C., 2017. Management of multiple nitrogen sources during wine fermentation by *Saccharomyces cerevisiae*. Appl. Environ. Microbiol. 83, 1–21. https://doi.org/10.1128/AEM.02617-16

Croft, T., Venkatakrishnan, P., Lin, S.-J.J., 2020. Nad^+ metabolism and regulation: Lessons from yeast. Biomolecules 10, 330. https://doi.org/10.3390/biom10020330

de Koning, W., van Dam, K., 1992. A method for the determination of changes of glycolytic metabolites in yeast on a subsecond time scale using extraction at neutral pH. Anal. Biochem. 204, 118–123. https://doi.org/10.1016/0003-2697(92)90149-2

Duncan, J.D., Setati, M.E., Divol, B., 2023. Redox cofactor metabolism in *Saccharomyces cerevisiae* and its impact on the production of alcoholic fermentation end-products. Food Res. Int. 163, 112276. https://doi.org/10.1016/j.foodres.2022.112276

Ehsani, M., Fernández, M.R., Biosca, J.A., Julien, A., Dequin, S., 2009. Engineering of 2,3-butanediol dehydrogenase to reduce acetoin formation by glycerol-overproducing, low-alcohol *Saccharomyces cerevisiae*. Appl. Environ. Microbiol. 75, 3196–3205. https://doi.org/10.1128/AEM.02157-08

Englezos, V., Rantsiou, K., Cravero, F., Torchio, F., Pollon, M., Fracassetti, D., Ortiz-Julien, A., Gerbi, V., Rolle, L., Cocolin, L., 2018. Volatile profile of white wines fermented with sequential inoculation of Starmerella bacillaris and *Saccharomyces cerevisiae*. Food Chem. 257, 350–360. https://doi.org/10.1016/j.foodchem.2018.03.018

Faijes, M., Mars, A.E., Smid, E.J., 2007. Comparison of quenching and extraction methodologies for metabolome analysis of *Lactobacillus plantarum*. Microb. Cell Fact. 6, 1–8. https://doi.org/10.1186/1475-2859-6-27

Fleet, G.H., 2003. Yeast interactions and wine flavour. Int. J. Food Microbiol. 86, 11–22. https://doi.org/10.1016/S0168-1605(03)00245-9

Gonzalez, R., Guindal, A.M., Tronchoni, J., Morales, P., 2021. Biotechnological approaches to lowering the ethanol yield during wine fermentation. Biomolecules 11. https://doi.org/10.3390/biom11111569

Grabowska, D., Chelstowska, A., 2003. The ALD6 gene product is indispensable for providing NADPH in yeast cells lacking glucose-6-phosphate dehydrogenase activity. J. Biol. Chem. 278, 13984–13988. https://doi.org/10.1074/jbc.M210076200

Harrison, R., Papp, B., Pál, C., Oliver, S.G., Delneri, D., 2007. Plasticity of genetic interactions in metabolic networks of yeast. Proc. Natl. Acad. Sci. 104, 2307–2312. https://doi.org/10.1073/pnas.0607153104

Haselbeck, R.J., McAlister-Henn, L., 1993. Function and expression of yeast mitochondrial NAD- and NADP-specific isocitrate dehydrogenases. J. Biol. Chem. 268, 12116–12122. https://doi.org/10.1016/S0021-9258(19)50315-5

Hazelwood, L.A., Daran, J.M., Van Maris, A.J.A., Pronk, J.T., Dickinson, J.R., 2008. The Ehrlich pathway

for fusel alcohol production: A century of research on *Saccharomyces cerevisiae* metabolism. Appl. Environ. Microbiol. 74, 2259–2266. https://doi.org/10.1128/AEM.02625-07

Henriques, D., Minebois, R., Mendoza, S.N., Macías, L.G., Pérez-Torrado, R., Barrio, E., Teusink, B., Querol, A., Balsa-Canto, E., 2021. A multiphase multiobjective dynamic genome-scale model shows different redox balancing among yeast species of the *Saccharomyces* genus in fermentation . mSystems 6. https://doi.org/10.1128/msystems.00260-21

Henschke, P.. ., Jiranek, V., 1993. Yeast - Metabolism of nitrogen compounds, in: Fleet, G.H. (Ed.), Wine Microbiology and Biotechnology. CRC Press, pp. 77–164.

Heux, S., Cachon, R., Dequin, S., 2006. Cofactor engineering in *Saccharomyces cerevisiae*: Expression of a H_2O-forming NADH oxidase and impact on redox metabolism. Metab. Eng. 8, 303–314. https://doi.org/10.1016/j.ymben.2005.12.003

Hou, J., Lages, N.F., Oldiges, M., Vemuri, G.N., 2009. Metabolic impact of redox cofactor perturbations in *Saccharomyces cerevisiae*. Metab. Eng. 11, 253–261. https://doi.org/10.1016/j.ymben.2009.05.001

Hranilovic, A., Gambetta, J.M., Schmidtke, L., Boss, P.K., Grbin, P.R., Masneuf-Pomarede, I., Bely, M., Albertin, W., Jiranek, V., 2018. Oenological traits of *Lachancea thermotolerans* show signs of domestication and allopatric differentiation. Sci. Rep. 8, 14812. https://doi.org/10.1038/s41598-018-33105-7

Ivit, N.N., Longo, R., Kemp, B., 2020. The effect of non-*Saccharomyces* and *Saccharomyces* non-*cerevisiae* yeasts on ethanol and glycerol levels in wine. Fermentation 6, 1–22. https://doi.org/10.3390/FERMENTATION6030077

Jagow, G., Klingenberg, M., 1970. Pathways of hydrogen in mitochondria of *Saccharomyces carlsbergensis*. Eur. J. Biochem. 12, 583–592. https://doi.org/10.1111/j.1432-1033.1970.tb00890.x

Jain, V.K., Divol, B., Prior, B.A., Bauer, F.F., 2012. Effect of alternative NAD^+-regenerating pathways on the formation of primary and secondary aroma compounds in a *Saccharomyces cerevisiae* glycerol-defective mutant. Appl. Microbiol. Biotechnol. 93, 131–141. https://doi.org/10.1007/s00253-011-3431-z

Jolly, N.P., Augustyn, O.P.H., Pretorius, I.S., 2003. The effect of non-*Saccharomyces* yeasts on fermentation and wine quality. South African J. Enol. Vitic. 24, 8–10. https://doi.org/10.21548/24-2-2638

Jolly, N.P., Varela, C., Pretorius, I.S., 2014. Not your ordinary yeast: Non-*Saccharomyces* yeasts in wine production uncovered. FEMS Yeast Res. 14, 215–237. https://doi.org/10.1111/1567-1364.12111

Kulkarni, C.A., Brookes, P.S., 2019. Cellular compartmentation and the redox/nonredox functions of NAD^+. Antioxid. Redox Signal. 31, 623–642. https://doi.org/10.1089/ars.2018.7722

Labuschagne, P.W.J., Rollero, S., Divol, B., 2021. Comparative uptake of exogenous thiamine and subsequent metabolic footprint in *Saccharomyces cerevisiae* and *Kluyveromyces marxianus* under simulated oenological conditions. Int. J. Food Microbiol. 354. https://doi.org/10.1016/j.ijfoodmicro.2021.109206

Lane, M.M., Morrissey, J.P., 2010. *Kluyveromyces marxianus*: A yeast emerging from its sister's shadow. Fungal Biol. Rev. 24, 17–26. https://doi.org/10.1016/j.fbr.2010.01.001

Larsson, C., Påhlman, I.L., Ansell, R., Rigoulet, M., Adler, L., Gustafsson, L., 1998. The importance of

the glycerol 3-phosphate shuttle during aerobic growth of *Saccharomyces cerevisiae*. Yeast 14, 347–357. https://doi.org/10.1002/(SICI)1097-0061(19980315)14:4<347::AID-YEA226>3.0.CO;2-9

Legras, J.L., Galeote, V., Bigey, F., Camarasa, C., Marsit, S., Nidelet, T., Sanchez, I., Couloux, A., Guy, J., Franco-Duarte, R., Marcet-Houben, M., Gabaldon, T., Schuller, D., Sampaio, J.P., Dequin, S., 2018. Adaptation of *S. cerevisiae* to fermented food environments reveals remarkable genome plasticity and the footprints of domestication. Mol. Biol. Evol. 35, 1712–1727. https://doi.org/10.1093/molbev/msy066

Li, Y.-F.F., Bao, W.-G.G., 2007. Why do some yeast species require niacin for growth? Different modes of NAD synthesis. FEMS Yeast Res. 7, 657–664. https://doi.org/10.1111/j.1567-1364.2007.00231.x

Lilly, M., Bauer, F.F., Styger, G., Lambrechts, M.G., Pretorius, I.S., 2006. The effect of increased branched-chain amino acid transaminase activity in yeast on the production of higher alcohols and on the flavour profiles of wine and distillates. FEMS Yeast Res. 6, 726–743. https://doi.org/10.1111/j.1567-1364.2006.00057.x

Loader, C., 2013. Local Regression, Likelihood and Density Estimation.

Marsit, S., Dequin, S., 2015. Diversity and adaptive evolution of *Saccharomyces* wine yeast: a review. FEMS Yeast Res. 15, fov067. https://doi.org/10.1093/femsyr/fov067

Mbuyane, L.L., de Kock, M., Bauer, F.F., Divol, B., 2018. *Torulaspora delbrueckii* produces high levels of C_5 and C_6 polyols during wine fermentations. FEMS Yeast Res. 18. https://doi.org/10.1093/femsyr/foy084

Morales, P., Rojas, V., Quirós, M., Gonzalez, R., 2015. The impact of oxygen on the final alcohol content of wine fermented by a mixed starter culture. Appl. Microbiol. Biotechnol. 99, 3993–4003. https://doi.org/10.1007/s00253-014-6321-3

Morata, A., Loira, I., Tesfaye, W., Bañuelos, M.A., González, C., Suárez Lepe, J.A., 2018. *Lachancea thermotolerans* applications in wine technology. Fermentation 4. https://doi.org/10.3390/fermentation4030053

Nielsen, J., 2003. It Is all about metabolic fluxes. J. Bacteriol. 185, 7031–7035. https://doi.org/10.1128/JB.185.24.7031-7035.2003

Nissen, T.L., Anderlund, M., Nielsen, J., Villadsen, J., Kielland-Brandt, M.C., 2001. Expression of a cytoplasmic transhydrogenase in *Saccharomyces cerevisiae* results in formation of 2-oxoglutarate due to depletion of the NADPH pool. Yeast 18, 19–32. https://doi.org/10.1002/1097-0061(200101)18:1<19::AID-YEA650>3.0.CO;2-5

Oura, E., 1977. Reaction products of yeast fermentations. Process Biochemistry. Process Biochem. 12, 19–35.

Outten, C.E., 2003. A novel NADH kinase is the mitochondrial source of NADPH in *Saccharomyces cerevisiae*. EMBO J. 22, 2015–2024. https://doi.org/10.1093/emboj/cdg211

Påhlman, I.L., Gustafsson, L., Rigoulet, M., Larsson, C., 2001. Cytosolic redox metabolism in aerobic chemostat cultures of *Saccharomyces cerevisiae*. Yeast 18, 611–620. https://doi.org/10.1002/yea.709

Pronk, J.T., Yde Steensma, H., van Dijken, J.P., 1996. Pyruvate metabolism in *Saccharomyces cerevisiae*. Yeast 12, 1607–1633. https://doi.org/10.1002/(SICI)1097-0061(199612)12:16<1607::AID-YEA70>3.0.CO;2-4

Quirós, M., Rojas, V., Gonzalez, R., Morales, P., 2014. Selection of non-*Saccharomyces* yeast strains for reducing alcohol levels in wine by sugar respiration. Int. J. Food Microbiol. 181, 85–91. https://doi.org/10.1016/j.ijfoodmicro.2014.04.024

Remize, F., Andrieu, E., Dequin, S., 2000. Engineering of the pyruvate dehydrogenase bypass in *Saccharomyces cerevisiae*: Role of the cytosolic Mg^{2+} and mitochondrial K^{+} acetaldehyde dehydrogenases Ald6p and Ald4p in acetate formation during alcoholic fermentation. Appl. Environ. Microbiol. 66, 3151–3159. https://doi.org/10.1128/AEM.66.8.3151-3159.2000

Richard, P., Teusink, B., Westerhoff, H. V, van Dam, K., 1993. Around the growth phase transition *S. cerevisiae*'s make-up favours sustained oscillations of intracellular metabolites. FEBS Lett. 318, 80–82. https://doi.org/10.1016/0014-5793(93)81332-T

Rigoulet, M., Aguilaniu, H., Avéret, N., Bunoust, O., Camougrand, N., Grandier-Vazeille, X., Larsson, C., Pahlman, I.L., Manon, S., Gustafsson, L., 2004. Organization and regulation of the cytosolic NADH metabolism in the yeast *Saccharomyces cerevisiae*. Mol. Cell. Biochem. 256–257, 73–81. https://doi.org/10.1023/b:mcbi.0000009888.79484.fd

Rollero, S., Bloem, A., Camarasa, C., Sanchez, I., Ortiz-Julien, A., Sablayrolles, J.M., Dequin, S., Mouret, J.R., 2015. Combined effects of nutrients and temperature on the production of fermentative aromas by *Saccharomyces cerevisiae* during wine fermentation. Appl. Microbiol. Biotechnol. 99, 2291–2304. https://doi.org/10.1007/s00253-014-6210-9

Rollero, S., Bloem, A., Ortiz-Julien, A., Bauer, F.F., Camarasa, C., Divol, B., 2019. A comparison of the nitrogen metabolic networks of *Kluyveromyces marxianus* and *Saccharomyces cerevisiae*. Environ. Microbiol. 21, 4076–4091. https://doi.org/10.1111/1462-2920.14756

Sadineni, V., Kondapalli, N., Reddy Obulam, V.S., 2012. Effect of co-fermentation with *Saccharomyces cerevisiae* and *Torulaspora delbrueckii* or *Metschnikowia pulcherrima* on the aroma and sensory properties of mango wine. Ann. Microbiol. 62, 1353–1360. https://doi.org/10.1007/s13213-011-0383-6

Sáez, M.J., Lagunas, R., 1976. Determination of intermediary metabolites in yeast. Critical examination of the effect of sampling conditions and recommendations for obtaining true levels. Mol. Cell. Biochem. 13, 73–78. https://doi.org/10.1007/BF01837056

Saint-Prix, F., Bönquist, L., Dequin, S., 2004. Functional analysis of the ALD gene family of *Saccharomyces cerevisiae* during anaerobic growth on glucose: the $NADP^{+}$-dependent Ald6p and Ald5p isoforms play a major role in acetate formation. Microbiology 150, 2209–2220. https://doi.org/10.1099/mic.0.26999-0

Sazanov, L.A., Jackson, J.B., 1994. Proton-translocating transhydrogenase and NAD- and NADP-linked isocitrate dehydrogenases operate in a substrate cycle which contributes to fine regulation of the tricarboxylic acid cycle activity in mitochondria. FEBS Lett. 344, 109–116. https://doi.org/10.1016/0014-5793(94)00370-X

Shekhawat, K., Bauer, F.F., Setati, M.E., 2020. The transcriptomic response of a wine strain of *Lachancea thermotolerans* to oxygen deprivation. FEMS Yeast Res. 20, 1–11. https://doi.org/10.1093/femsyr/foaa054

Swiegers, J.H., Bartowsky, E.J., Henschke, P.A., Pretorius, I.S., 2005. Yeast and bacterial modulation of wine aroma and flavour. Aust. J. Grape Wine Res. 11, 139–173. https://doi.org/10.1111/j.1755-0238.2005.tb00285.x

Tondini, F., Onetto, C.A., Jiranek, V., 2020. Early adaptation strategies of *Saccharomyces cerevisiae* and *Torulaspora delbrueckii* to co-inoculation in high sugar grape must-like media. Food

Microbiol. 90, 103463. https://doi.org/10.1016/j.fm.2020.103463

Torrea, D., 2003. Production of volatile compounds in the fermentation of chardonnay musts inoculated with two strains of *Saccharomyces cerevisiae* with different nitrogen demands. Food Control 14, 565–571. https://doi.org/10.1016/S0956-7135(02)00146-9

van Dijken, J.P., Scheffers, W.A., 1986. Redox balances in the metabolism of sugars by yeasts. FEMS Microbiol. Lett. 32, 199–224. https://doi.org/10.1016/0378-1097(86)90291-0

van Hoek, M.J.A., Merks, R.M.H., 2012a. Redox balance is key to explaining full vs. partial switching to low-yield metabolism. BMC Syst. Biol. 6. https://doi.org/10.1186/1752-0509-6-22

Vicente, J., Kelanne, N., Rodrigo-Burgos, L., Navascués, E., Calderón, F., Santos, A., Marquina, D., Yang, B., Benito, S., 2023. Influence of different *Lachancea thermotolerans* strains in the wine profile in the era of climate challenge. FEMS Yeast Res. 23, 1–8. https://doi.org/10.1093/femsyr/foac062

Zwietering, M.H., Jongenburger, I., Rombouts, F.M., van 't Riet, K., 1990. Modeling of the Bacterial Growth Curve. Appl. Environ. Microbiol. 56, 1875–1881. https://doi.org/10.1128/aem.56.6.1875-1881.1990

Table 1: Wine yeast strains investigated in this study and their codes used throughout this manuscript.

Yeast species	Strain	Code	Supplier/Culture Collection
Saccharomyces cerevisiae	Lalvin EC1118™	Sc1	Lallemand
Torulaspora delbrueckii	Level^2 Biodiva™	Td1	Lallemand
Lachancea thermotolerans	Level^2 Laktia™	Lt1	Lallemand
Lachancea thermotolerans	IWBT Y1240	LtY1240	SAGWRI
Kluyveromyces marxianus	IWBT Y885	KmY885	SAGWRI
Starmerella bacillaris	MTF 3768	SbMTF3768	CIRM
Starmerella bacillaris	MTF 3800	SbMTF3800	CIRM
Metschnikowia pulcherrima	Level^2 Flavia™	Mp1	Lallemand

SAGWRI: South African Grape and Wine Research Institute, Stellenbosch University, South Africa; CIRM: Centre International de Ressources Microbiennes (France), and Lallemand: Lallemand Inc. (Montreal, QC, Canada)

Table 2: Comparison of different fermentation kinetics parameters between strains.

Parameter	Sc1	Td1	Lt1	LtY1240	KmY885	SbMTF3768	SbMTF3800	Mp1
Rmax (g/L/h)	1.01 ±0.01 ^{A}	0.84 ±0.02 ^{BC}	0.80 ±0.03 ^{C}	0.87 ±0.01 ^{B}	0.21 ±0.02 ^{F}	0.33 ±0.01 ^{D}	0.32 ±0.04 ^{D}	0.25 ±0.01 ^{E}
Time to reach Rmax (h)	32.5 ±0.50 ^{D}	42.3 ±1.26 ^{C}	43.2 ±1.53 ^{C}	40.2 ±0.76 ^{C}	89.6 ±0.00 ^{A}	59.2 ±2.25 ^{B}	61.3 ±1.61 ^{B}	31.5 ±0.50 ^{D}
CO_2 at Rmax (g/L)	18.92 ±0.18 ^{A}	19.51 ±0.46 ^{A}	19.69 ±0.05 ^{A}	19.29 ±0.58 ^{A}	8.25 ±0.29 ^{B}	8.86 ±0.41 ^{B}	8.99 ±0.88 ^{B}	4.71 ±0.18 ^{C}
Rate at 30 g/L CO_2 (g/L/h)	0.95 ±0.12 ^{A}	0.77 ±0.02 ^{B}	0.81 ±0.05 ^{B}	0.89 ±0.03 ^{AB}	0.20 ±0.01 ^{C}	0.21 ±0.02 ^{C}	0.21 ±0.03 ^{C}	0.08 ±0.00 ^{C}
Rate at 60 g/L CO_2 (g/L/h)	0.74 ±0.02 ^{A}	0.41 ±0.01 ^{B}	0.29 ±0.02 ^{C}	0.27 ±0.01 ^{C}	0.13 ±0.01 ^{D}	*p.n.r.*	*p.n.r.*	*p.n.r.*
Lag Time (h)	13.03 ±0.64 ^{CD}	17.47 ±0.51 ^{C}	17.17 ±1.05 ^{C}	14.67 ±0.12 ^{CD}	55.80 ±5.07 ^{A}	30.10 ±1.11 ^{B}	31.17 ±0.35 ^{B}	10.20 ±0.00 ^{D}
Max CO_2 (g/L)	98.11 ±0.93 ^{A}	94.00 ±0.98 ^{B}	83.76 ±0.96 ^{C}	93.14 ±0.97 ^{B}	85.02 ±1.26 ^{C}	51.72 ±1.05 ^{D}	52.50 ±0.59 ^{D}	42.75 ±0.85 ^{E}
Duration (h)	264.63 ±0.00 ^{H}	374.07 ±0.00 ^{F}	374.03 ±0.00 ^{G}	432.92 ±0.00 ^{C}	807.85 ±0.01 ^{A}	422.01 ±0.00 ^{D}	421.97 ±0.00 ^{E}	469.97 ±0.00 ^{B}

Results represent the mean ± SD for three replicates. Means in the same row with the same superscript letter(s) are not significantly different ($p < 0.05$)

p.n.r. – point not reached.

Rmax – maximum rate of CO_2 production. Time to reach Rmax – the time (h) at which maximum rate of fermentation is reached. CO_2 at Rmax – CO_2 (g/L) produced at Rmax. Rate at 30 and/or 60 g/L – Rate (g/L/h) when the yeast reaches 30 and/or 60 g/L CO_2. Lag time – the time (h) from the beginning of fermentation to the point at which 1 g/L cumulative CO_2 has been produced.

Table 3: Dry biomass (g/L) during synthetic grape must fermentation by wine yeast strains.

Fermentation phase	Sc1	Td1	Lt1	LtY1240	KmY885	SbMTF3768	SbMTF3800	Mp1
30 g/L CO_2	3.31 ± 0.11 ^{A}	2.88 ± 0.27 ^{A}	2.83 ± 0.52 ^{A}	3.01 ± 0.09 ^{A}	1.42 ± 0.01 ^{B}	1.69 ± 0.22 ^{A}	1.11 ± 0.06 ^{B}	1.11 ± 0.04 ^{B}
60 g/L CO2	3.85 ± 0.15 ^{A}	3.64 ± 0.10 ^{A}	3.26 ± 0.04 ^{B}	3.03 ± 0.05 ^{B}	1.21 ± 0.07 ^{C}	*p.n.r.*	*p.n.r.*	*p.n.r.*

Results represent the mean ± SD for three replicates. Means in the same row with the same superscript letter(s) are not significantly different ($p < 0.05$). *p.n.r.* – point not reached.

Table 4: Primary metabolites (central carbon metabolites or from sugar metabolism) quantified at the end of fermentation (g/L). Fermentations were stopped when the CO_2 production rate was at or less than 0.02 g/L/h for 48 h.

Metabolite (g/L)	Sc1	Td1	Lt1	LtY1240	KmY885	SbMTF3768	SbMTF3800	Mp1
Ethanol	95.03 ± 0.97 ^{A}	93.25 ± 1.12 ^{A}	81.62 ± 0.64 ^{C}	89.55 ± 0.75 ^{B}	76.08 ± 1.89 ^{D}	47.58 ± 0.05 ^{E}	47.84 ± 1.12 ^{E}	38.06 ± 0.33 ^{F}
Glycerol	5.95 ± 0.23 ^{BC}	8.77 ± 0.42 ^{AB}	8.70 ± 0.14 ^{AB}	5.28 ± 3.30 ^{C}	9.84 ± 0.08 ^{A}	7.40 ± 0.19 ^{ABC}	7.82 ± 0.30 ^{ABC}	4.78 ± 0.13 ^{C}
Acetate	0.51 ± 0.04 ^{B}	0.10 ± 0.01 ^{DE}	0.34 ± 0.01 ^{C}	0.20 ± 0.13 ^{CDE}	1.95 ± 0.03 ^{A}	0.15 ± 0.02 ^{DE}	0.25 ± 0.06 ^{CD}	0.09 ± 0.01 ^{E}
Succinate	0.99 ± 0.04 ^{C}	2.18 ± 0.20 ^{A}	1.25 ± 0.02 ^{B}	1.17 ± 0.01 ^{BC}	1.25 ± 0.01 ^{B}	0.46 ± 0.01 ^{D}	0.48 ± 0.02 ^{D}	0.67 ± 0.04 ^{D}
Lactate	0.18 ± 0.01 ^{B}	0.09 ± 0.00 ^{B}	6.51 ± 0.29 ^{A}	0.17 ± 0.11 ^{B}	0.07 ± 0.01 ^{B}	0.06 ± 0.00 ^{B}	0.06 ± 0.01 ^{B}	0.05 ± 0.00 ^{B}
Acetoin	0.00 ± 0.00 ^{B}	0.00 ± 0.00 ^{B}	0.03 ± 0.02 ^{AB}	0.00 ± 0.00 ^{B}	0.00 ± 0.00 ^{B}	0.03 ± 0.02 ^{AB}	0.05 ± 0.02 ^{A}	0.00 ± 0.00 ^{B}
Butanediol	0.30 ± 0.04 ^{A}	0.30 ± 0.04 ^{A}	0.00 ± 0.00 ^{C}	0.35 ± 0.10 ^{A}	0.23 ± 0.01 ^{AB}	0.13 ± 0.01 ^{BC}	0.11 ± 0.10 ^{BC}	0.00 ± 0.00 ^{C}
Residual sugars	0.52 ± 0.19 ^{E}	0.82 ± 0.13 ^{E}	20.08 ± 2.38 ^{D}	7.95 ± 5.20 ^{E}	33.73 ± 1.72 ^{C}	96.18 ± 0.97 ^{B}	90.29 ± 2.43 ^{B}	116.47 ± 3.55 ^{A}

Results represent the mean ± SD for three replicates. Means in the same row with the same superscript letter(s) are not significantly different ($p < 0.05$).

Table 5: Concentrations of secondary metabolites (mg/L) produced by the various strains, and, residual sugars is sum of glucose and fructose measured at the end of fermentation for each strain.

	Sc1	Td1	Lt1	LtY1240	KmY885	SbMTF3768	SbMTF3800	Mp1
Residual sugars (g/L)	0.52 ± 0.19 ^{E}	0.82 ± 0.13 ^{E}	20.08 ± 2.38 ^{D}	7.95 ± 5.20 ^{E}	33.73 ± 1.72 ^{C}	90.29 ± 2.43 ^{B}	96.18 ± 0.97 ^{B}	116.47 ± 3.55 ^{A}
Higher alcohols (mg/L)								
Propanol	30.59 ±1.84 ^{B}	31.13 ± 3.69 ^{B}	56.17 ± 1.96 ^{A}	59.23 ± 3.36 ^{A}	32.09 ± 1.67 ^{B}	29.10 ± 2.10 ^{B}	31.52 ± 3.25 ^{B}	8.21 ± 0.80 ^{C}
Isobutanol	68.92 ±5.54 ^{E}	86.01 ±18.39 ^{DE}	121.60 ±10.21 ^{CD}	66.96 ± 2.98 ^{E}	80.96 ± 2.18 ^{E}	195.49 ±20.32 ^{B}	130.05 ±16.70 ^{C}	245.87 ± 17.37 ^{A}
Isoamyl Alcohol	395.96 ± 38.45 ^{A}	334.63 ± 60.09 ^{A}	380.91 ± 54.98 ^{A}	317.68 ± 7.19 ^{A}	124.37 ± 4.98 ^{BC}	48.45 ± 11.49 ^{C}	53.22 ± 4.36 ^{C}	204.84 ± 22.35 ^{B}
Methionol	1.82 ± 0.47 ^{B}	2.43 ± 0.08 ^{B}	15.23 ± 1.98 ^{A}	18.89 ± 7.26 ^{A}	6.13 ± 0.92 ^{B}	1.75 ± 0.24 ^{B}	5.53 ± 1.25 ^{B}	1.50 ± 0.27 ^{B}
2-Phenylethanol	165.99 ± 13.68 ^{A}	154.08 ± 22.76 ^{A}	87.52 ± 12.47 ^{B}	82.94 ± 5.89 ^{B}	10.67 ± 0.09 ^{C}	22.50 ± 8.82 ^{C}	27.14 ± 1.09 ^{C}	191.32 ± 32.40 ^{A}
Acetate esters (mg/L)								
Isoamyl acetate	2.79 ± 0.09 ^{A}	0.09 ± 0.01 ^{C}	1.19 ± 0.22 ^{B}	0.96 ± 0.05 ^{B}	1.16 ± 0.07 ^{B}	0.00 ± 0.00 ^{C}	0.00 ± 0.00 ^{C}	0.15 ± 0.03 ^{C}
2-Phenylethyl acetate	27.25 ± 1.70 ^{A}	0.00 ± 0.00 ^{B}	22.55 ± 11.31 ^{A}	0.00 ± 0.00 ^{B}	8.90 ± 0.07 ^{B}	0.00 ± 0.00 ^{B}	0.00 ± 0.00 ^{B}	0.00 ± 0.00 ^{B}
2-Methylbutyl acetate	0.55 ± 0.02 ^{A}	0.01 ± 0.00 ^{C}	0.30 ± 0.05 ^{B}	0.24 ± 0.02 ^{B}	0.29 ± 0.02 ^{B}	0.00 ± 0.00 ^{C}	0.00 ± 0.00 ^{C}	0.03 ± 0.01 ^{C}
Propyl Acetate	0.05 ± 0.00 ^{C}	0.02 ± 0.00 ^{D}	0.08 ± 0.00 ^{B}	0.06 ± 0.01 ^{C}	0.24 ± 0.02 ^{A}	0.00 ± 0.00 ^{D}	0.00 ± 0.00 ^{D}	0.01 ± 0.00 ^{D}
2-Methylpropyl acetate	0.09 ± 0.01 ^{C}	0.03 ± 0.01 ^{DE}	0.24 ± 0.01 ^{A}	0.12 ± 0.02 ^{B}	0.24 ± 0.01 ^{A}	0.04 ± 0.01 ^{D}	0.00 ± 0.01 ^{E}	0.07 ± 0.01 ^{C}
Yield of converstion Ratio $= \frac{\sum acetate\ ester}{\sum Higher\ alcohol} \times 100$	0.78	0.07	0.20	0.19	2.97	0.01	0.00	0.03
Ethyl Esters (mg/L)								
Ethyl lactate	1.70 ± 0.16 ^{B}	0.76 ± 0.03 ^{B}	61.21 ± 1.77 ^{A}	0.73 ± 0.04 ^{B}	0.69 ± 0.04 ^{B}	1.60 ± 0.18 ^{B}	1.09 ± 0.31 ^{B}	0.20 ± 0.03 ^{B}
Ethyl propionoate	0.17 ± 0 .00 ^{B}	0.00 ± 0.00 ^{D}	0.00 ± 0.00 ^{CD}	0.00 ± 0.00 ^{D}	0.19 ± 0.01 ^{A}	0.01 ± 0.01 ^{CD}	0.00 ± 0.00 ^{D}	0.02 ± 0.00 ^{C}
Ethyl isobutyrate	0.00 ± 0.00 ^{C}	0.03 ± 0.01 ^{B}	0.11 ± 0.02 ^{A}	0.04 ± 0.00 ^{B}	0.04 ± 0.00 ^{B}	0.03 ± 0.01 ^{B}	0.00 ± 0.00 ^{C}	0.00 ± 0.00 ^{C}
Ethyl butanoate	0.30 ± 0.01 ^{B}	0.35 ± 0.02 ^{A}	0.06 ± 0.00 ^{CDE}	0.05 ± 0.01 ^{DEF}	0.01 ± 0 .00 ^{F}	0.10 ± 0.01 ^{C}	0.08 ± 0.03 ^{CD}	0.02 ± 0.00 ^{EF}
Ethyl hexanoate	0.87 ± 0.06 ^{A}	0.16 ± 0.01 ^{B}	0.05 ± 0.00 ^{CD}	0.06 ± 0.00 ^{C}	0.01 ± 0.00 ^{CD}	0.00 ± 0.00 ^{D}	0.00 ± 0.00 ^{D}	0.00 ± 0.00 ^{CD}
Ethyl octanoate	1.03 ± 0.03 ^{A}	0.15 ± 0.02 ^{B}	0.07 ± 0.01 ^{C}	0.09 ± 0.01 ^{C}	0.03 ± 0.00 ^{D}	0.00 ± 0.00 ^{D}	0.02 ± 0.00 ^{D}	0.01 ± 0.01 ^{D}
Ethyl decanoate	0.99 ± 0.09 ^{A}	0.11 ± 0.05 ^{B}	0.19 ± 0.05 ^{B}	0.74 ± 0.31 ^{A}	0.04 ± 0.00 ^{B}	0.02 ± 0.00 ^{B}	0.03 ± 0.00 ^{B}	0.03 ± 0.00 ^{B}
Ethyl dodecanoate	0.19 ± 0.03 ^{A}	0.10 ± 0.01 ^{AB}	0.03 ± 0.05 ^{BC}	0.10 ± 0.01 ^{AB}	0.10 ± 0.00 ^{BC}	0.06 ± 0.05 ^{BC}	0.03 ± 0.05 ^{BC}	0.00 ± 0.00 ^{C}
Fusel and medium-chain fatty acids (mg/L)								
Propanoic acid	3.32 ± 0.50 ^{CDE}	7.25 ± 2.73 ^{B}	14.16 ± 1.74 ^{A}	5.61 ± 0.50 ^{BC}	4.68 ± 0.26 ^{BCD}	3.76 ± 0.67 ^{CDE}	1.96 ± 0.53 ^{DE}	0.49 ± 0.05 ^{E}
2-methylbutanoic acid	41.73 ± 14.64 ^{A}	2.09 ± 0.24 ^{B}	0.49 ± 0.03 ^{B}	0.27 ± 0.02 ^{B}	0.67 ± 0.03 ^{B}	0.13 ± 0.01 ^{B}	0.11 ± 0.00 ^{B}	0.09 ± 0.00 ^{B}
3-methylbutanoic acid	40.67 ± 2.72 ^{A}	1.96 ± 0.30 ^{B}	1.60 ± 2.33 ^{B}	0.79 ± 1.05 ^{B}	0.24 ± 0.01 ^{B}	0.31 ± 0.38 ^{B}	0.06 ± 0.05 ^{B}	0.10 ± 0.01 ^{B}
Butanoic acid	31.01 ± 0.86 ^{A}	6.37 ± 5.38 ^{B}	2.00 ± 2.85 ^{B}	1.59 ± 2.59 ^{B}	0.44 ± 0.01 ^{B}	0.20 ± 0.08 ^{B}	0.31 ± 0.02 ^{B}	0.26 ± 0.11 ^{B}
Hexanoic acid	123.30 ± 14.98 ^{A}	1.76 ± 1.42 ^{B}	0.25 ± 0.11 ^{B}	2.00 ± 2.98 ^{B}	0.40 ± 0.01 ^{B}	1.11 ± 1.62 ^{B}	0.19 ± 0.01 ^{B}	0.25 ± 0.05 ^{B}
Octanoic acid	9.49 ± 1.01 ^{A}	1.43 ± 0.21 ^{B}	0.93 ± 0.12 ^{BC}	1.23 ± 0.28 ^{B}	0.16 ± 0.02 ^{C}	0.41 ± 0.02 ^{BC}	0.43 ± 0.02 ^{BC}	0.39 ± 0.04 ^{BC}
Decanoic acid	2.26 ± 0.47 ^{A}	0.15 ± 0.02 ^{B}	0.46 ± 0.21 ^{B}	2.07 ± 0.81 ^{A}	0.22 ± 0.01 ^{B}	0.09 ± 0.01 ^{B}	0.09 ± 0.02 ^{B}	0.18 ± 0.15 ^{B}
Dodecanoic acid	0.23 ± 0.03 ^{A}	0.16 ± 0.00 ^{AB}	0.15 ± 0.00 ^{B}	0.21 ± 0.02 ^{AB}	0.19 ± 0.00 ^{AB}	0.22 ± 0.01 ^{AB}	0.21 ± 0.06 ^{AB}	0.00 ± 0.00 ^{C}

Results represent the mean ± SD for three replicates. Means in the same row with the same superscript letter(s) are not significantly different ($p < 0.05$).

Figure captions

Figure 1: Fermentation kinetics of eight wine yeast strains. A: CO_2 production curves of the different wine yeast strains fermented in synthetic grape must with 200 g/L total sugars and 200 mg/L YAN at 22°C. The values are displayed as mean and standard deviations from triplicate experiments. B: The rate of CO_2 production by various wine yeast strains during fermentation. The dashed line represents the end of fermentation threshold, which we defined it as when the rate of CO_2 production is ≤ 0.02 g/L/h for at least 48 h. The values are displayed as mean from triplicate experiments. Standard deviations are not displayed to enhance visual clarity but are all lower than 5%. (B). Sc1 (Peach), Td1 (Dark Orange), Lt1 (Blue), LtY1240 (Light Green), KmY885 (Light Blue), SbMTF3768 (Rose Pink), SbMTF3800 (Red), and Mp1 (Dark Green).

Figure 2: A: Total NADP(H) levels in pmol/10^7 cells were also measured at the same time points as total NAD(H) and are presented by physiological stage. B: Total NAD(H) levels in mmol/cell at different physiological phases in wine yeast during fermentation. A ratio of more than 1.0x indicates a more oxidized system (NAD^+ or $NADP^+$ dominance), while a ratio less than 1.0x defines a more reduced system (NADH or NADPH dominance). Letters above the histograms denote statistically significant differences ($p < 0.05$) in Total [NADH] and [NADPH] values between strains at specific time points, namely 50% OD (entry into exponential phase of CO_2 production), 30 g/L CO_2 (entry into stationary growth phase and maximum population for faster strains and in KmY885). Meanwhile, 65% CO_2 production corresponds to the mid-stationary growth phase and was sampled at 60 g/L CO_2 production for the faster strains and 30 g/L CO_2 for Mp1, SbMTF3768, and SbMTF3800 only. The data are representative of three independent biological replicates and two technical replicates per sampling point.

Figure 3: Comparison of primary metabolite production yield between the yeast strains investigated in this study. The mean values and standard deviations from triplicate experiments are presented, with the data reflecting three independent biological replicates. The error bars represent the standard deviation. Letters above the histograms indicate statistically significant differences ($p < 0.05$).

Figure 4: Principal component analysis biplot of the aroma compounds that were quantified at the end of fermentation (analysed according to the intermediates or product of their respective metabolic pathways) and the various strains. Aroma compounds are analysed based on the keto acid precursors involved in the metabolic pathways that produce these compounds, with the exception of medium-chain fatty acids (MCFAs), which are derived from acetyl-CoA metabolism; as such, MCFAs are analysed based on this substrate. αKMBA - α-keto-γ-(methylthio)butyrate.

Supplementary material

Table S1: Composition of a synthetic must with 200 g/L of sugars, 200 mg/L of assimilable nitrogen, and 5 mg/L of phytosterols. The pH is adjusted to 3.3 with a 10 M NaOH solution.

Compounds	**Quantity per liter**
Glucose	100 g
Fructose	100 g
Malic acid	6 g
Citric acid	6 g
Potassium phosphate (KH_2PO_4)	0.75 g
Potassium sulfate (K_2SO_4)	0.5 g
Magnesium sulfate heptahydrate ($MgSO_4$, $7H_2O$)	0.25 g
Calcium chloride dihydrate ($CaCl_2$, $2H_2O$)	0.155 g
Sodium chloride (NaCl)	0.2 g
Ammonium chloride (NH_4Cl)	0.216 g
Amino acid stock solution (Table S2)	6.16 mL
Stock solution of trace elements (Table S3)	1 mL
Stock solution of vitamins (Table S4)	10 mL
Phytosterols stock solution	0.25 mL
Iron stock solution (20g/L $FeCl_3$ $6H_2O$)	1 mL

Table S2: Composition of the amino acid stock solution. This solution was stored at -20 °C.

Amino acid	Quantity per liter
Aspartic acid	3.4 g
Glutamic acid	9.4 g
Alanine	11.1 g
Arginine	28.6 g
Cysteine	1 g
Glutamine	38.6 g
Glycine	1.4 g
Histidine	2.5 g
Isoleucine	2.5 g
Leucine	3.7 g
Lysine	1.3 g
Methionine	2.4 g
Phenylalanine	2.9 g
Proline	46.8 g
Serine	6 g
Threonine	5.8 g
Tryptophan	13.7 g
Tyrosine	1.4 g
Valine	3.4 g

Table S3: Composition of the stock solution of trace elements. The solution is sterilized by filtration at 0.22 µm and stored at 4°C.

Compounds	Quantity per liter
Manganese sulfate monohydrate	4 g
Zinc sulfate heptahydrate	4 g
Copper sulfate pentahydrate	1 g
Potassium iodide	1 g
Cobalt chloride hexahydrate	0.4 g
Boric acid	1 g
Ammonium heptamolybdate	1 g

Table S4: Composition of the vitamin stock solution. This solution is stored at -20 °C.

Vitamin compounds	Quantity per liter
Myo-inositol	2 g
Calcium pantothenate	0.15 g
Thiamine hydrochloride	0.025 g
Nicotinic acid	0.2 g
Pyridoxine	0.025 g
Biotin	3 mL

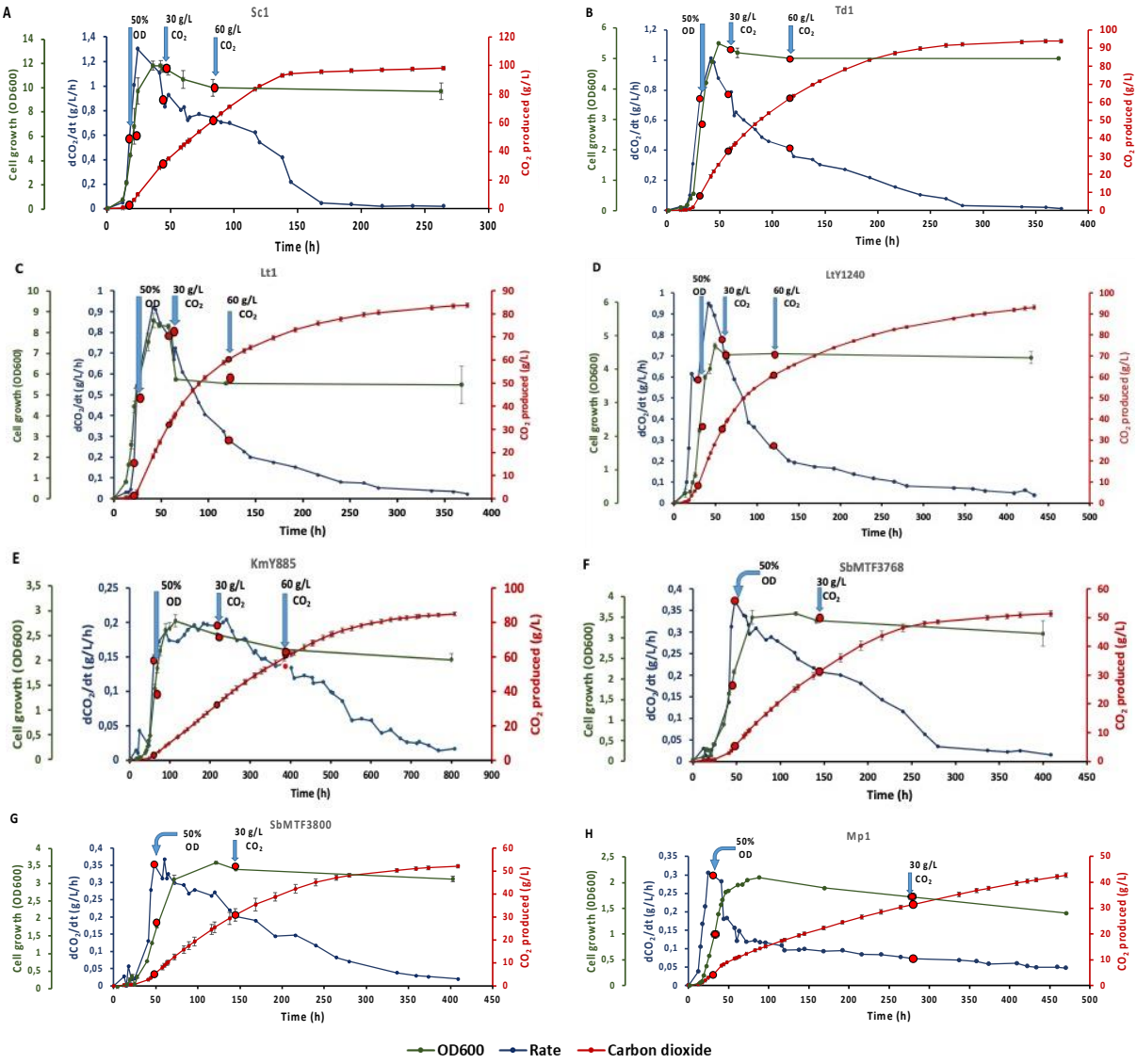

Figure S1: Progress of cell growth at OD600 (Green), rate of CO_2 production (g/L/h) (Dark Blue), and CO_2 production (g/L) (Red), Sc1 (A), Td1 (B), Lt1 (C), LtY1240 (D), KmY885 (E), SbMTF3768 (F), SbMTF3800 (G), and Mp1 (H).

Table S5: Determination of growth kinetics and extrapolation of 50% population sampling point at OD600 for cofactors measurements

Parameter	Sc1	Td1	Lt1	LtY1240	KmY885	SbMTF3768	SbMTF3800	Mp1
Growth Rate, μ (h^{-1})	0.34 ± 0.07 ^{A}	0.27 ± 0.04 ^{AB}	0.27 ± 0.01 ^{AB}	0.22 ± 0.01 ^{BC}	0.12 ± 0.01 ^{D}	0.11 ± 0.01 ^{D}	0.10 ± 0.02 ^{D}	0.17 ± 0.01 ^{CD}
50% OD	20 h	32 h	20 h	30 h	60 h	45 h	48 h	32 h

Results represent the mean ± SD for three replicates. Means in the same row with the same letter are not significantly different ($p < 0.05$)

Table S6: Production of redox sinks during fermentation (g/L).

Metabolite (g/L)	Sc1	Td1	Lt1	LtY1240	KmY885	SbMTF3768	SbMTF3800	Mp1
Concentration of metabolites when fermentations reached 50% OD								
Ethanol	11.24 ± 0.10 ^{B}	10.55 ± 0.05 ^{C}	3.50 ± 0.14 ^{G}	12.00 ± 0.36 ^{A}	3.14 ± 0.20 ^{G}	6.10 ± 0.05 ^{E}	7.76 ± 0.46 ^{D}	4.59 ± 0.23 ^{F}
Glycerol	1.54 ± 0.04 ^{A}	1.75 ± 0.01 ^{A}	0.49 ± 0.03 ^{E}	1.83 ± 0.07 ^{A}	0.58 ± 0.01 ^{E}	1.24 ± 0.02 ^{C}	1.51 ± 0.13 ^{B}	0.77 ± 0.05 ^{D}
Acetate	0.17 ± 0.00 ^{A}	0.02 ± 0.02 ^{B}	0.00 ± 0.00 ^{B}	0.02 ± 0.01 ^{B}	0.00 ± 0.00 ^{B}	0.00 ± 0.00 ^{B}	0.00 ± 0.00 ^{B}	0.02 ± 0.01 ^{B}
Succinate	0.11 ± 0.02 ^{B}	0.18 ± 0.00 ^{A}	0.00 ± 0.00 ^{D}	0.14 ± 0.01 ^{B}	0.00 ± 0.00 ^{D}	0.00 ± 0.00 ^{D}	0.04 ± 0.02 ^{CD}	0.05 ± 0.01 ^{C}
Lactate	0.07 ± 0.00 ^{A}	0.04 ± 0.00 ^{C}	0.00 ± 0.00 ^{E}	0.05 ± 0.00 ^{B}	0.00 ± 0.00 ^{E}	0.00 ± 0.00 ^{E}	0.00 ± 0.00 ^{E}	0.02 ± 0.00 ^{D}
Concentration of metabolites when fermentations reached 30 g/L CO_2								
Ethanol	35.40 ± 1.29 ^{AB}	35.20 ± 0.26 ^{AB}	34.98 ± 2.65 ^{AB}	37.05 ± 0.23 ^{A}	31.24 ± 1.35 ^{AB}	30.66 ± 2.73 ^{B}	30.63 ± 2.37 ^{B}	34.04 ± 3.36 ^{AB}
Glycerol	3.65 ± 0.16 ^{C}	4.93 ± 0.13 ^{B}	5.45 ± 0.47 ^{AB}	4.71 ± 0.03 ^{B}	6.38 ± 0.23 ^{A}	5.39 ± 0.56 ^{AB}	5.63 ± 0.58 ^{AB}	4.63 ± 0.37 ^{BC}
Acetate	0.39 ± 0.02 ^{B}	0.03 ± 0.03 ^{C}	0.11 ± 0.01 ^{C}	0.09 ± 0.01 ^{C}	1.19 ± 0.06 ^{A}	0.01 ± 0.00 ^{C}	0.04 ± 0.03 ^{C}	0.15 ± 0.11 ^{C}
Succinate	0.44 ± 0.02 ^{D}	0.79 ± 0.04 ^{A}	0.71 ± 0.07 ^{AB}	0.57 ± 0.00 ^{C}	0.71 ± 0.07 ^{AB}	0.23 ± 0.02 ^{E}	0.23 ± 0.01 ^{E}	0.61 ± 0.02 ^{BC}
Lactate	0.16 ± 0.01 ^{B}	0.05 ± 0.00 ^{B}	6.60 ± 0.44 ^{A}	0.06 ± 0.00 ^{B}	0.03 ± 0.00 ^{B}	0.04 ± 0.00 ^{B}	0.05 ± 0.00 ^{B}	0.05 ± 0.00 ^{B}
Concentration of metabolites when fermentations reached 60 g/L CO_2								
Ethanol	63.90 ± 2.42 ^{A}	63.08 ± 1.47 ^{A}	61.50 ± 0.62 ^{A}	61.75 ± 0.72 ^{A}	57.69 ± 0.41 ^{B}	*p.n.r.*	*p.n.r.*	*p.n.r.*
Glycerol	5.06 ± 0.20 ^{E}	7.32 ± 0.34 ^{C}	7.83 ± 0.13 ^{B}	6.30 ± 0.01 ^{D}	8.74 ± 0.10 ^{A}	*p.n.r.*	*p.n.r.*	*p.n.r.*
Acetate	0.45 ± 0.01 ^{B}	0.06 ± 0.06 ^{D}	0.23 ± 0.01 ^{C}	0.19 ± 0.01 ^{C}	1.75 ± 0.03 ^{A}	*p.n.r.*	*p.n.r.*	*p.n.r.*
Succinate	0.68 ± 0.03 ^{C}	1.65 ± 0.15 ^{A}	1.04 ± 0.03 ^{B}	0.92 ± 0.01 ^{B}	1.04 ± 0.01 ^{B}	*p.n.r.*	*p.n.r.*	*p.n.r.*
Lactate	0.20 ± 0.01 ^{B}	0.08 ± 0.01 ^{B}	6.53 ± 0.36 ^{A}	0.08 ± 0.00 ^{B}	0.05 ± 0.00 ^{B}	*p.n.r.*	*p.n.r.*	*p.n.r.*

p.n.r. - point not reached

Results represent the mean ± SD for three replicates. Means in the same row with the same subscript letter(s) are not significantly different ($p < 0.05$)

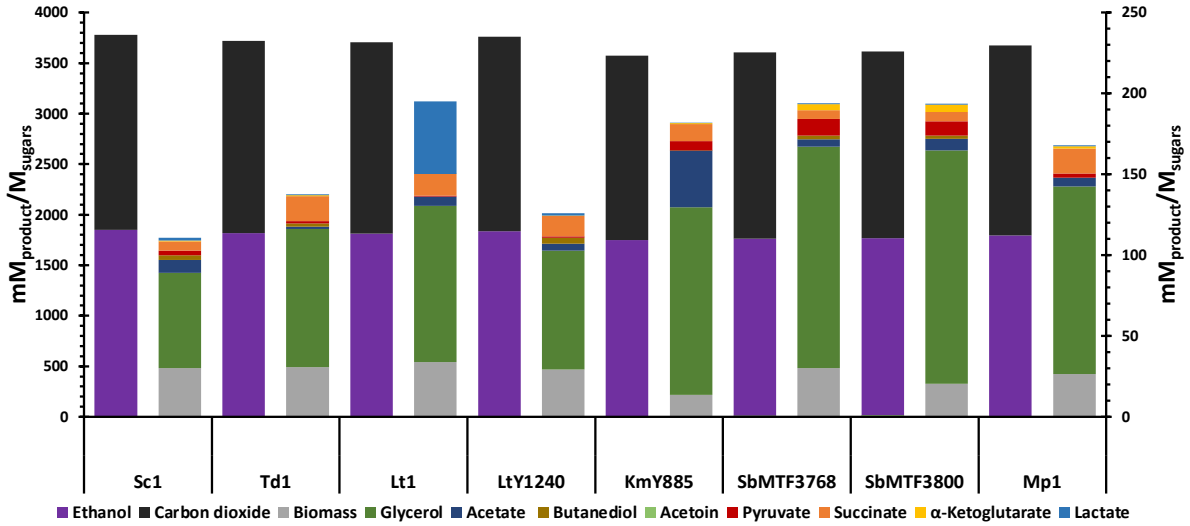

Figure S2: The carbon balance in $mM_{product}/M_{sugars}$ of each strain was compared at the end of fermentation. The major primary metabolites of alcoholic fermentation (ethanol and carbon dioxide) are represented by stacked bars on the left y-axis, while the by-products (such as biomass, glycerol, acetate, 2,3-butanediol, acetoin, pyruvate, succinate, α-ketoglutarate, and lactate) are shown on the right y-axis as stacked bars. All values represent the quantity of carbon (in mM/L) used for each product per mol/L of consumed carbon (from glucose and fructose, which is referred to as glucose in this study).

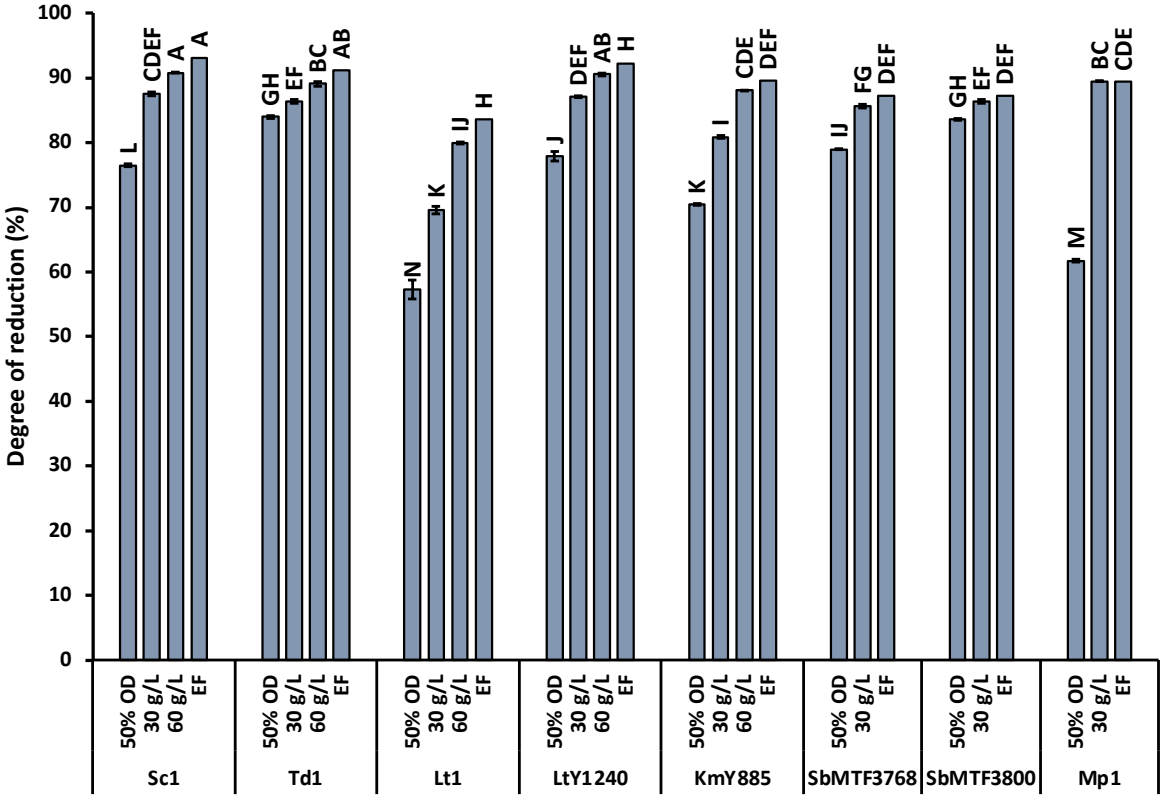

Figure S4: The dynamics of the degree of reduction in wine yeasts during fermentation.

Figure 1

Click here to access/download;Figure;Figure_1_Figure_1_Fermentation_Kinet

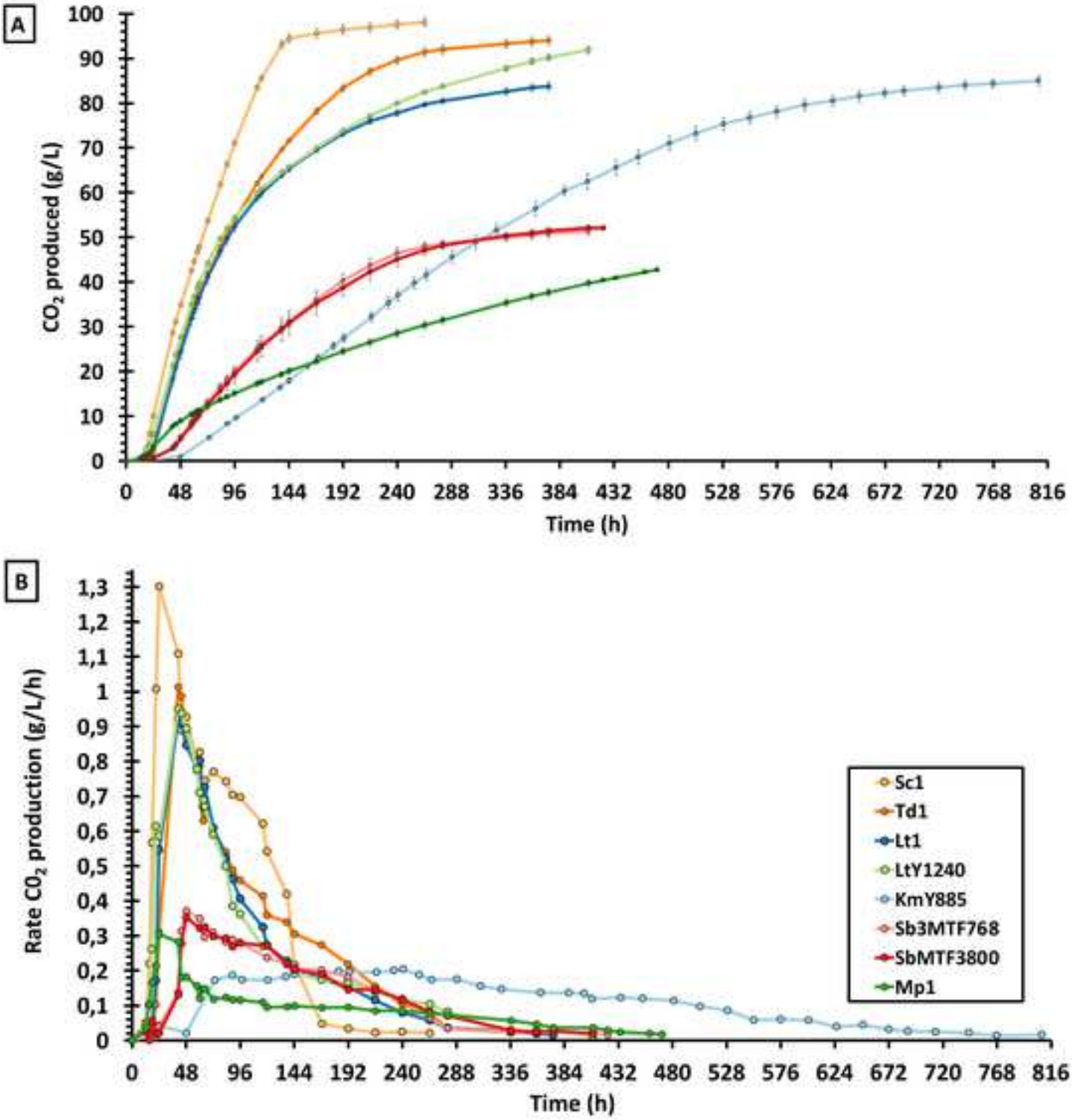

Figure 2

Click here to access/download;Figure;Figure_2_Figure_2_Total_NAD(H)_et_N

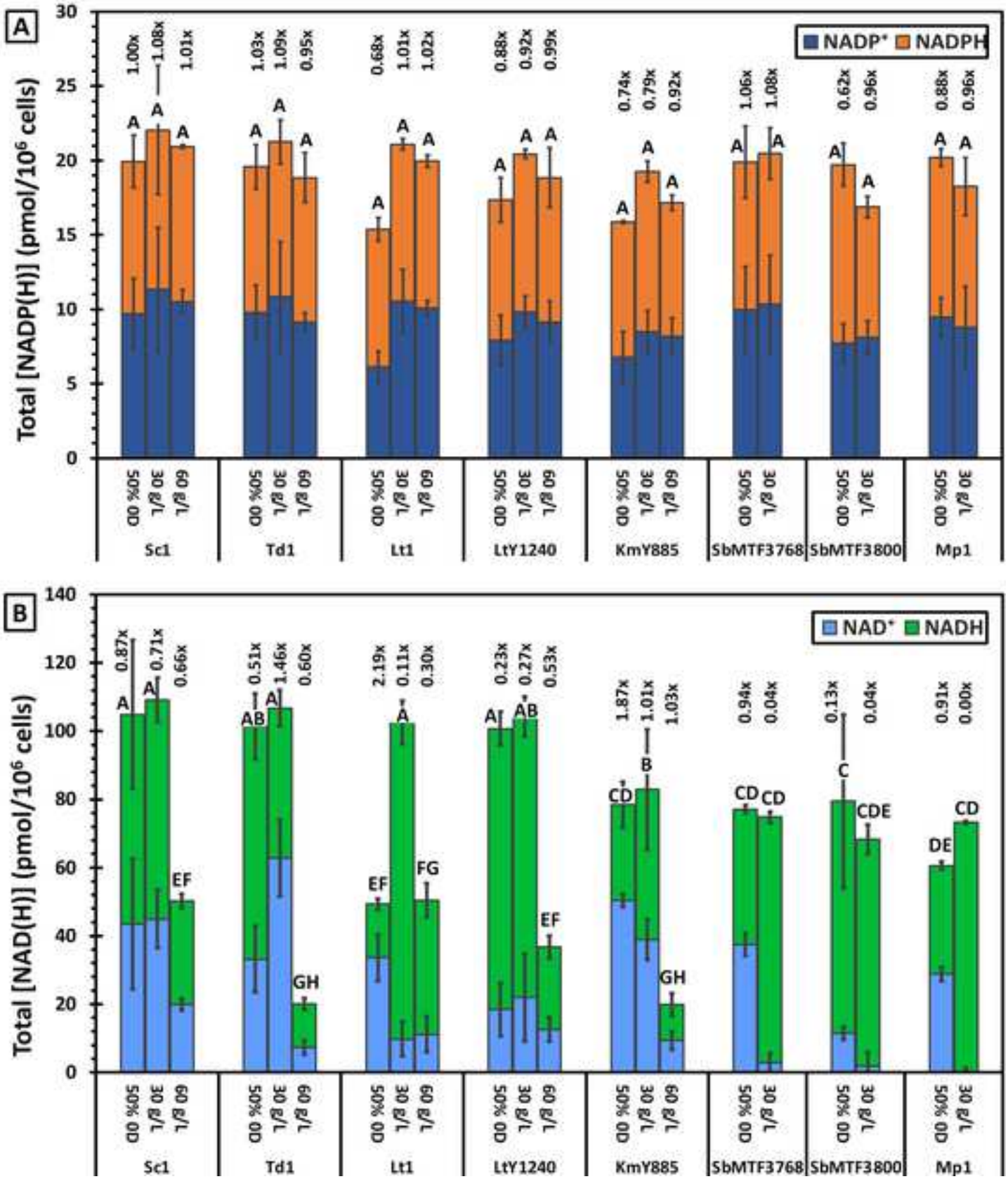

Figure 3

Click here to access/download;Figure;Figure_3_Figure_3_CCM_Yields.tif

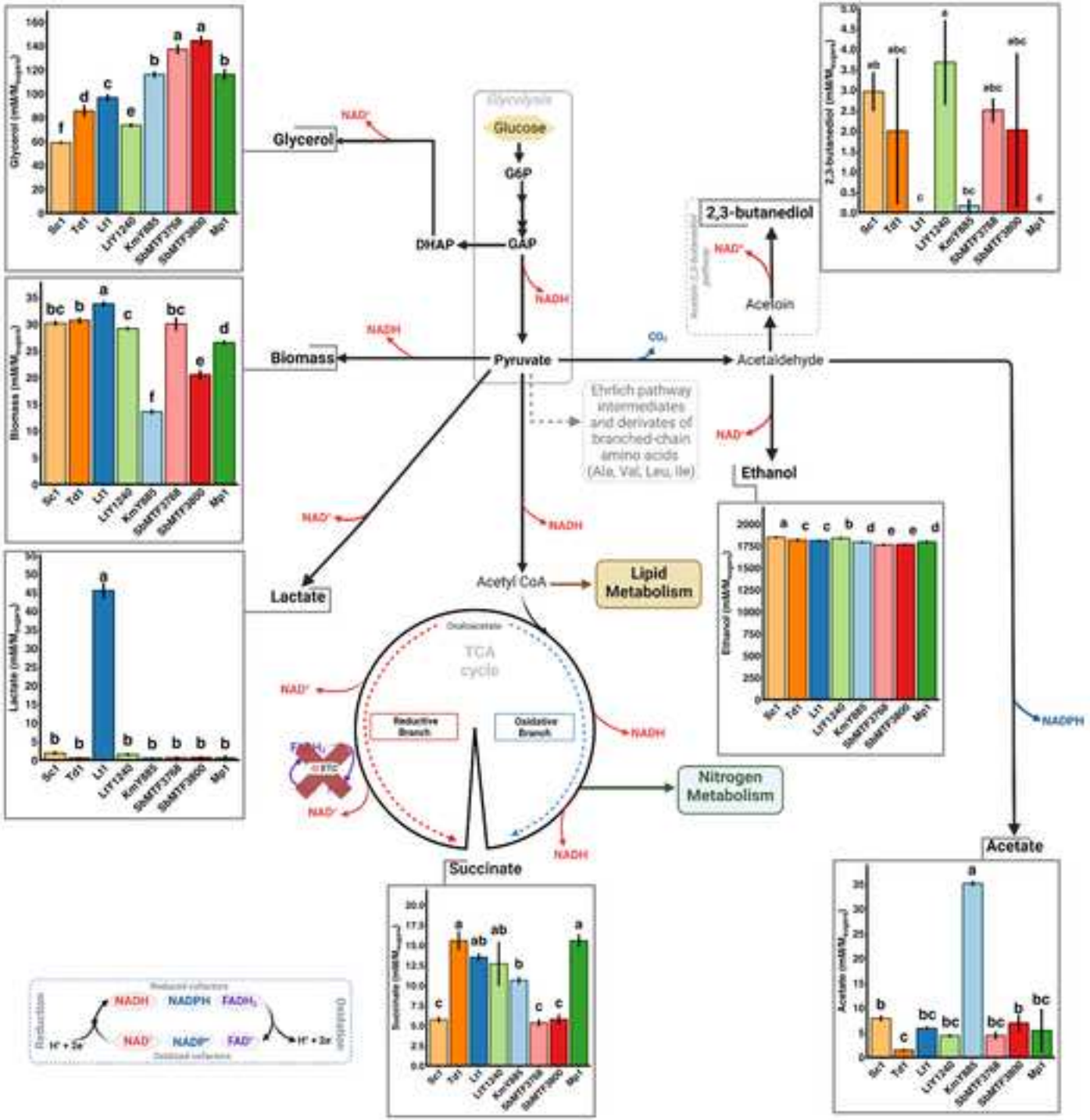

Figure 4

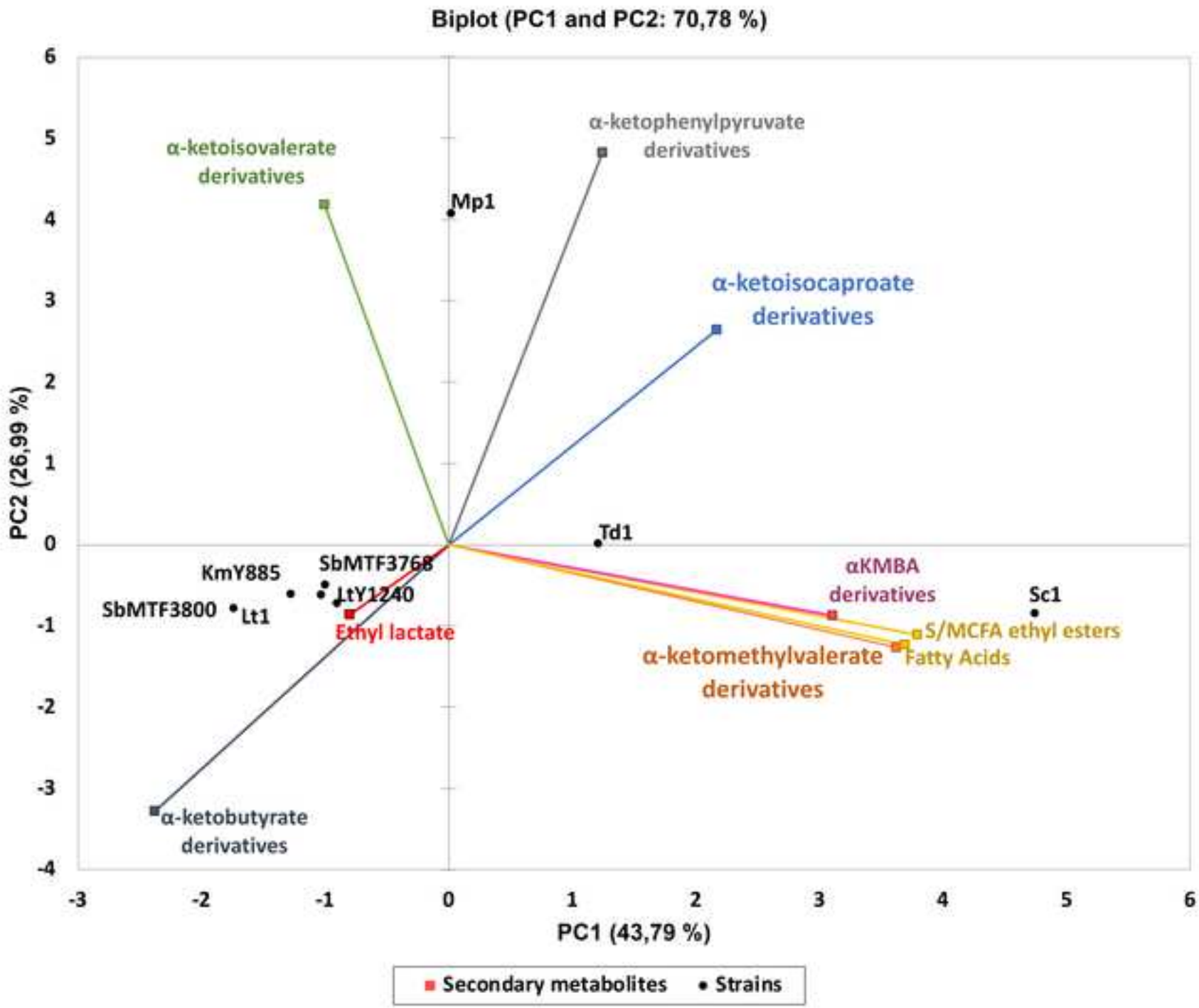

Declaration of competing interest

The authors state that they have no financial conflicts of interest or personal relationships that could have influenced the work reported in this paper.